

DTIC FILE COPY

NSWC TR 87-368

AD-A193 978

# **CORROSION/DETERIORATION OF FUEL TANK MATERIALS WETTED IN METHANOLIC ELECTROLYTES**

BY W. A. FERRANDO  
RESEARCH AND TECHNOLOGY DEPARTMENT

15 DECEMBER 1987

Approved for public release, distribution is unlimited.

DTIC  
ELECTE  
APR 12 1988  
S D



**NAVAL SURFACE WARFARE CENTER**

Dahlgren, Virginia 22448-5000 • Silver Spring, Maryland 20903-5000

88 4 11 1988

UNCLASSIFIED

SECURITY CLASSIFICATION OF THIS PAGE

## REPORT DOCUMENTATION PAGE

1a. REPORT SECURITY CLASSIFICATION UNCLASSIFIED			1b. RESTRICTIVE MARKINGS		
2a. SECURITY CLASSIFICATION AUTHORITY			3. DISTRIBUTION/AVAILABILITY OF REPORT Approved for public release; distribution is unlimited.		
2b. DECLASSIFICATION/DOWNGRADING SCHEDULE					
4. PERFORMING ORGANIZATION REPORT NUMBER(S) NSWC TR 87-368			5. MONITORING ORGANIZATION REPORT NUMBER(S)		
6a. NAME OF PERFORMING ORGANIZATION Naval Surface Warfare Center		6b. OFFICE SYMBOL (If applicable) R32	7a. NAME OF MONITORING ORGANIZATION		
6c. ADDRESS (City, State, and ZIP Code) White Oak Laboratory 10901 New Hampshire Avenue Silver Spring, MD 20903-5000			7b. ADDRESS (City, State, and ZIP Code)		
8a. NAME OF FUNDING / SPONSORING ORGANIZATION		8b. OFFICE SYMBOL (If applicable)	9. PROCUREMENT INSTRUMENT IDENTIFICATION NUMBER		
8c. ADDRESS (City, State, and ZIP Code)			10. SOURCE OF FUNDING NUMBERS		
		PROGRAM ELEMENT NO.	PROJECT NO.	TASK NO. 7G73TCF01	WORK UNIT ACCESSION NO.
11. TITLE (Include Security Classification) Corrosion/Deterioration of Fuel Tank Materials Wetted in Methanolic Electrolytes					
12. PERSONAL AUTHOR(S) Ferrando, W. A.					
13a. TYPE OF REPORT		13b. TIME COVERED FROM 1986 TO 1987		14. DATE OF REPORT (Year, Month, Day) 1987, December, 15	
				15. PAGE COUNT 57	
16. SUPPLEMENTARY NOTATION					
17. COSATI CODES			18. SUBJECT TERMS (Continue on reverse if necessary and identify by block number)		
FIELD	GROUP	SUB-GROUP			
11	10, 11		Methanolic Electrolyte, Galvanic Corrosion, Crevice Corrosion, Polymer O-ring Degradation, 6061-T6 Al Alloy Corrosion		
19. ABSTRACT (Continue on reverse if necessary and identify by block number)					
<p>A question has been raised concerning the stability of various fuel wetted device structural materials over a prolonged storage period in methanol based electrolytes. Accelerated corrosion tests were designed to study this problem. These included potentiodynamic scanning, galvanic couple and elevated temperature corrosion studies. The observation of physical property changes was employed for the nonmetallic component.</p> <p>The materials examined were: anodized and unanodized 6061-T6 aluminum, 5052-32 anodized aluminum, 1018 bare and zinc plated steel, and an ethylene-propylene O-ring material.</p> <p>The aluminum showed immediate very severe autocatalytic pitting in the electrolyte containing 30 percent <math>\text{CCl}_4</math> during the potentiodynamic scan. This fuel mixture thus proved itself completely incompatible with the requirements. The anodized aluminum</p> <p style="text-align: right;">(Cont.)</p>					
20. DISTRIBUTION/AVAILABILITY OF ABSTRACT <input checked="" type="checkbox"/> UNCLASSIFIED/UNLIMITED <input type="checkbox"/> SAME AS RPT. <input type="checkbox"/> DTIC USERS			21. ABSTRACT SECURITY CLASSIFICATION UNCLASSIFIED		
22a. NAME OF RESPONSIBLE INDIVIDUAL Dr. William A. Ferrando		22b. TELEPHONE (Include Area Code) (202) 394-3527		22c. OFFICE SYMBOL R32	

DD FORM 1473, 84 MAR

83 APR edition may be used until exhausted.

All other editions are obsolete

SECURITY CLASSIFICATION OF THIS PAGE

★ U.S. Government Printing Office: 1985-839-612

0102-1.F-014-6602

UNCLASSIFIED

## Block 19. (Cont.)

showed less than 1 mil/year corrosion rate in the second fuel (100 percent undried reagent grade methanol) with indication of prompt surface passivation. The unanodized aluminum showed a somewhat higher initial corrosion rate with some minor shallow pitting. Passivation was not yet evident at 24 hours immersion.

A galvanic corrosion couple of the coated steel and anodized aluminum showed anodic behavior of the steel through the first 400 hours until the zinc plating dissolved. Subsequently, the aluminum became anodic with a limited corrosion current of about 1.3 nanoamps/cm<sup>2</sup>, corresponding to <.001 mils/year.

An elevated temperature sealed crevice corrosion test showed no corrosion at the fluid-exposed O-ring groove. Corrosion due to the presence of surrounding moisture was observed in the caps of the test containers up to the atmospheric side of the O-ring grooves.

Finally, observation and a simple tensile test revealed that the O-ring itself had softened considerably. The vessels had not yet leaked appreciably. Use of the given O-ring material, however, places a limit on long term storage life of the device.

## FOREWORD

Most Navy corrosion research is directed rightly toward the investigation of the durability of metals and system performance in the marine environment. It is sometimes required, however, to design systems which must contain organic fluids or fuels in metal reservoirs for long periods prior to or between uses. A long shelf life under extreme temperature variations often is required.

Behavior unanticipated from the relative inertness ordinarily observed with these substances sometimes occurs. This report documents an investigation of one such system containing methanol-based fuels.

Approved by:

*James F. Goff*  
JAMES F. GOFF, Acting Head  
Materials Division

Accession For	
NTIS GRA&I	<input checked="" type="checkbox"/>
DTIC TAB	<input type="checkbox"/>
Unannounced	<input type="checkbox"/>
Justification	
By	
Distribution/	
Availability Codes	
Dist	Avail and/or Special
A-1	<div style="border: 1px solid black; border-radius: 50%; padding: 5px; display: inline-block;">         6710 GOLF INSPECTED 4       </div>

## CONTENTS

<u>Chapter</u>		<u>Page</u>
1	INTRODUCTION.....	1
2	BACKGROUND.....	3
3	PART I: POTENTIODYNAMIC TESTS .....	7
	EXPERIMENTAL.....	7
	MEASUREMENTS IN THE FUEL MIXTURE.....	8
	THEORY OF PITTING CORROSION.....	11
	APPLICATION TO CASE OF ALUMINUM IN FUEL MIXTURE....	11
	MEASUREMENTS IN PURE METHANOL.....	14
4	PART II: GALVANIC CORROSION.....	23
	BACKGROUND.....	23
	EXPERIMENTAL.....	23
	RESULTS.....	26
5	PART III: CREVICE CORROSION.....	35
	BACKGROUND.....	35
	EXPERIMENTAL.....	35
	ISSUES CONCERNING THE SEALED CAVITY CORROSION TEST...	37
	RESULTS.....	44
6	SUMMARY.....	49
	REFERENCES.....	51
	DISTRIBUTION.....	(1)

## ILLUSTRATIONS

<u>Figure</u>		<u>Page</u>
1	FUEL WETTED CAVITY COMPONENTS.....	4
2	POTENTIODYNAMIC SCAN OF UNANODIZED 6061-T6 ALUMINUM IN FUEL MIXTURE CONTAINING CCl <sub>4</sub> .....	9
3	SURFACE OF UNANODIZED 6061-T6 ALUMINUM BEFORE AND AFTER POTENTIODYNAMIC SCANS IN FUEL MIXTURE CONTAINING CCl <sub>4</sub> .....	10
4	SCHEMATIC REPRESENTATIONS OF PITTING CORROSION AND CREVICE CORROSION.....	12
5	ANODIZED 6061-T6 ALUMINUM SURFACE BEFORE AND AFTER POTENTIODYNAMIC SCANS AND 24 HOUR IMMERSION IN METHANOL.....	15
6	ZINC-PLATED STEEL SURFACE BEFORE AND AFTER POTENTIO- DYNAMIC SCANS AND 24 HOUR IMMERSION IN METHANOL.....	16
7	UNANODIZED 6061-T6 ALUMINUM SURFACE BEFORE AND AFTER POTENTIODYNAMIC SCANS AND 24 HOUR IMMERSION IN METHANOL.....	17
8	POTENTIODYNAMIC SCAN OF UNANODIZED 6061-T6 ALUMINUM IN METHANOL.....	18
9	POTENTIODYNAMIC SCAN OF ZINC-PLATED STEEL IN METHANOL.....	19
10	COLD-MOUNTED ZINC-PLATED STEEL AND ANODIZED 6061-T6 ALUMINUM SAMPLES IN THE TRUE FUEL WETTED AREA RATIO, BEFORE GALVANIC CORROSION TEST.....	25
11	ALUMINUM-STEEL GALVANIC COUPLE CORROSION SCAN: GALVANIC CURRENT VERSUS TIME IN METHANOL.....	27

## ILLUSTRATIONS (Cont.)

<b>Figure</b>		<b>Page</b>
12	GALVANIC CURRENT DENSITY VERSUS TIME FOR ZINC-PLATED STEEL/6061-T6 ALUMINUM COUPLE IN METHANOL.....	28
13	CORROSION POTENTIAL $E_{\text{corr}}$ VERSUS TIME FOR ZINC-PLATED STEEL/6061-T6 ALUMINUM COUPLE IN METHANOL.....	29
14	GALVANIC CURRENT DENSITY VERSUS TIME FOR 1020 STEEL/6061-T6 ALUMINUM COUPLE IN 3.5% NaCl SOLUTION.....	30
15	ZINC-PLATED STEEL SURFACE BEFORE AND AFTER GALVANIC CORROSION TEST IN METHANOL.....	31
16	ANODIZED 6061-T6 ALUMINUM SURFACE BEFORE AND AFTER GALVANIC CORROSION TEST IN METHANOL.....	33
17	DESIGN CHART FOR INDUSTRIAL O-RING STATIC SEAL GLANDS..	36
18	1018 STEEL/6061-T6 ALUMINUM VESSELS FABRICATED FOR CREVICE CORROSION TEST IN METHANOL.....	38
19	ZINC-PLATED STEEL CAP, BEFORE AND AFTER CREVICE CORROSION TEST, ARGON FILL AND AIR FILL.....	39
20	O-RING CONTACT AREA OF UNANODIZED 6061-T6 ALUMINUM CONTAINER, BEFORE AND AFTER CREVICE CORROSION TEST.....	40
21	UNPLATED 1018 STEEL CAP BEFORE AND AFTER CREVICE CORROSION TEST.....	45

## TABLES

<u>Table</u>		<u>Page</u>
1	DESCRIPTIONS AND MATERIAL DESIGNATIONS OF TESTED COMPONENTS.....	7
2	CORROSION DATA ON TESTED METALS IN PURE METHANOL BY POTENTIODYNAMIC SCANNING.....	20
3	GALVANIC SERIES IN SEAWATER FOR VARIOUS METALS.....	24
4	CHEMICAL RESISTANCE OF VARIOUS ELASTOMERS.....	42
5	COMPARATIVE PROPERTIES OF O-RING MATERIALS.....	43
6	ELECTROLYTE LOSS DURING 70°C CREVICE CORROSION TEST.....	46
7	SOFTENING OF O-RING DURING 70°C CREVICE CORROSION TEST.....	46

## CHAPTER 1

### INTRODUCTION

The primary interest in corrosion by the Navy lies rightfully in concern for the performance of its many systems in the harsh marine atmospheric conditions in which they must operate. Here, the aerated chloride-rich environment is well known to produce and exacerbate many serious corrosion problems.

There are situations, however, in which components must be exposed to solvents or fuels, often at elevated storage temperature for extended periods before use. The tendency in these cases can be to ignore or minimize their potential for corrosion from a perception that they are generally non-conducting and quite inert. Indeed, contact of these fluids with most metals and polymers shows no short term attack. One purpose of this report is to show the often unanticipated corrosion effects which can occur with extended and elevated temperature storage.

## CHAPTER 2

## BACKGROUND

The aluminum alloy 6061-T6 and zinc plated steels are common structural fabrication materials for Navy hardware. The two contacting organic "electrolyte" fluids used in this study were a methanol based fuel mixture containing  $\text{CCl}_4$  (50% methanol, 30% carbon tetrachloride, 20% trimethylborate) and 100% reagent grade methanol (undried), respectively. Previous work has implicated such fluids as abettors of corrosive attack even on metals and alloys chosen for their corrosion resistance. Roques, et al.,<sup>1</sup> state that methanolic solutions containing some  $\text{Cl}^-$  were found to be more aggressive toward Zr, Ti, Ta and Cr than aqueous solutions of the same  $\text{Cl}^-$  concentration. Likewise, Singh and Banerjee<sup>2</sup> showed, in particular, that nickel does not exhibit passivity in methanol containing less than 0.5% water. They found that  $\text{Cl}^-$  ions induced pitting. Nickel, further, was observed to dissolve actively in methanol-HCl mixtures with restoration of passivity only upon the introduction of a sufficient quantity of water.

These examples illustrate the vulnerability of many metals, especially those dependent upon a protective oxide layer for their corrosion resistance, to organic solvents. In the present case, a minimum 5 year storage life (-65 to +160 °F) of the sealed fuel-tank system with negligible leakage and with the device remaining fully functional is required. Figure 1 shows the fuel wetted portion of the device. The zinc plated steel tank bottom (left), anodized aluminum walls, and O-rings are shown. Quick initial information was required on the overall corrosion performance for this configuration. Therefore, specific tests were devised for rapid results. The first phase of this program involved short term corrosion compatibility testing of the two fuels specified above as candidates for use in the subject device.

The emphasis was on extended storage of the vessel in an O-ring sealed condition under potentially harsh environmental conditions. Thus, it was recommended that the mechanisms of galvanic and crevice corrosion be investigated for this system. In addition to temperature extremes, the storage locker is subject to occasional seawater incursions. The effect of a moisture laden partially wetting atmosphere surrounding the tank also became a significant consideration and was incidentally treated. The containing vessel must retain its integrity and the fuel shall not have leaked or decomposed during the anticipated storage period. Any corrosion by the fuel or surrounding atmosphere which jeopardizes this integrity would be considered unacceptable.

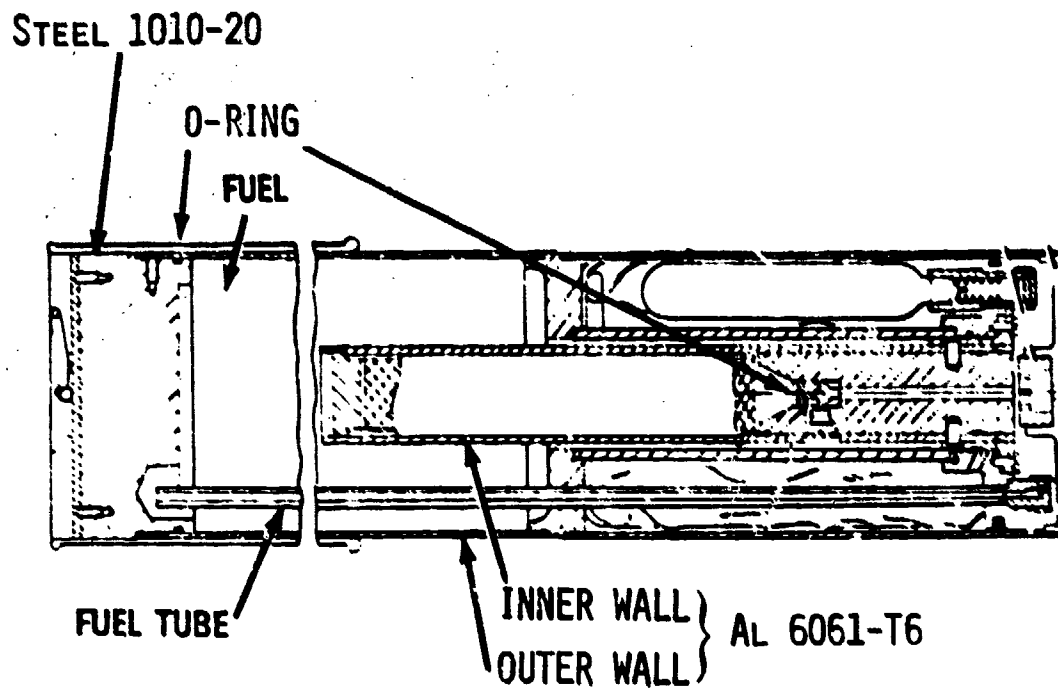


FIGURE 1. FUEL WETTED CAVITY COMPONENTS

It is significant to note that the upper limit of storage temperature is close to the atmospheric pressure boiling point of both fuels. Hence, the internal cavity pressure will approach 15 lbs/in<sup>2</sup> under this storage condition. While this pressure is not high enough to induce corrosion mechanisms such as stress cracking or inter-granular corrosion, it is enough to hasten the failure of a weakened vessel. In this eventuality, the flammable fluids will be propelled from the device with danger of fire and injury to personnel. In addition, the fuel cavity is gas pressurized during use. A fuel cavity sufficiently weakened by corrosion, therefore, could cause the device to malfunction during use.

## CHAPTER 3

## PART I: POTENTIODYNAMIC TESTS

## EXPERIMENTAL

Small samples of the aluminum and steel components of the device fuel tank were fitted with wire connections and cold mounted with a special plastic. Some aluminum samples were mechanically polished with a series of grits and finished with a fine oxide compound. The remaining aluminum and steel samples were left in their original anodized and zinc plated states, respectively. The mounted samples were masked to a 1 cm<sup>2</sup> exposed area with resistant epoxy paint. Table 1 gives the component descriptions and material designations for the items tested.

TABLE 1. DESCRIPTIONS AND MATERIAL DESIGNATIONS OF TESTED COMPONENTS

<u>COMPONENT</u>	<u>MATERIAL DESIGNATION</u>
Aluminum body section	6061-T6 aluminum (1.0%Mg, 0.6%Si, 0.25%Cr), anodized in accord with MIL-A8625 Type II, Class I. Also, unanodized samples of this aluminum alloy
Aluminum screen	5052-32 aluminum anodized as above
Steel nose section	1010-1020 steel, zinc plated in accord with ASTM B633-78, Class Fe/Zn 13, SC3 Type II
O-ring	Ethylene-propylene

The laboratory method of potentiodynamic scanning was chosen as that most likely to yield rapid information on the corrosion susceptibility of the metals in the two prospective fuels. The resulting data were supplemented extensively by optical photography. In the potentiodynamic (pd) method, a potential, referenced to an appropriate standard, is applied to the sample and slowly stepped from negative (cathodic) to positive (anodic) values. The response current

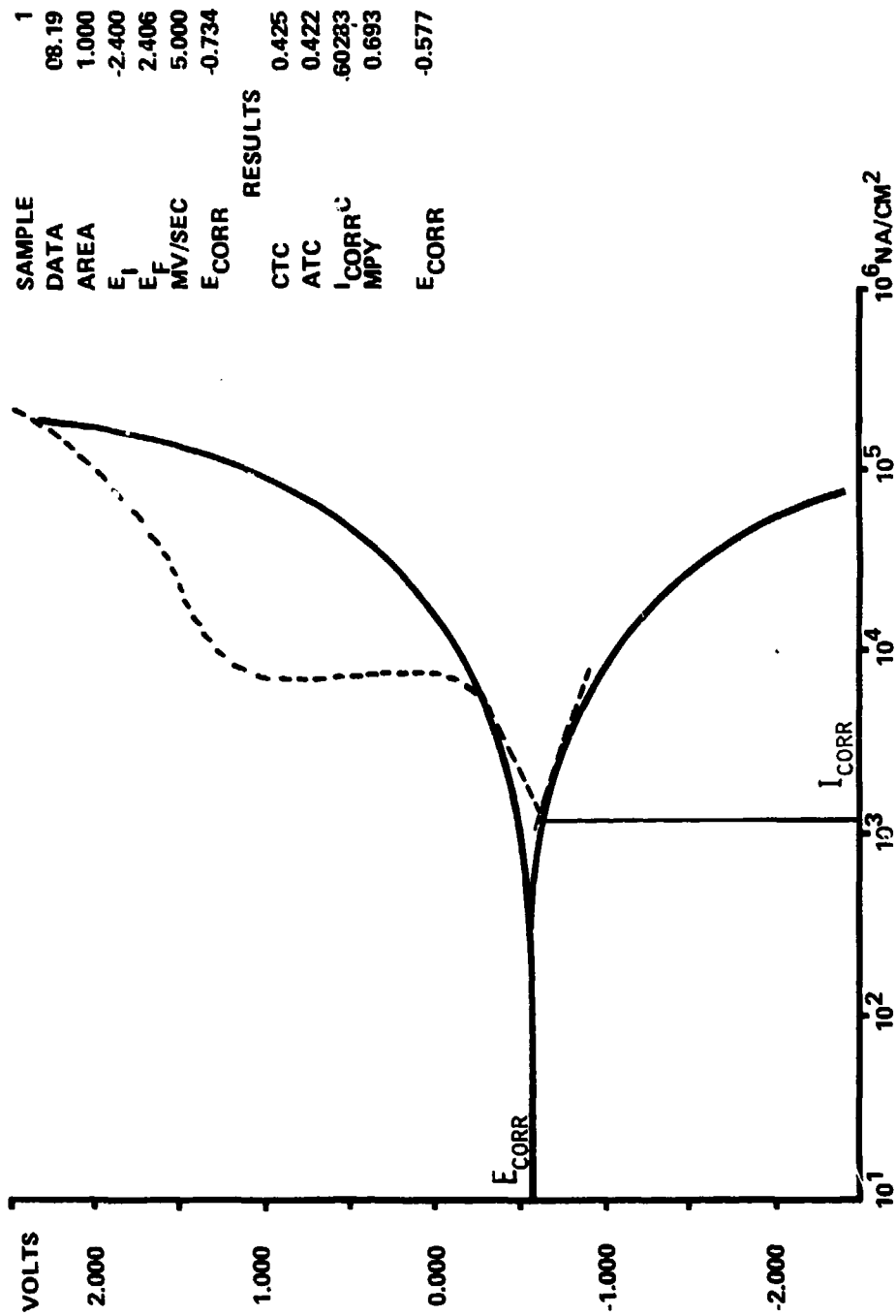
of the circuit is measured and recorded versus an inert counterelectrode. Corrosion characteristics of the sample in the electrolyte can be determined from the shape of this curve.

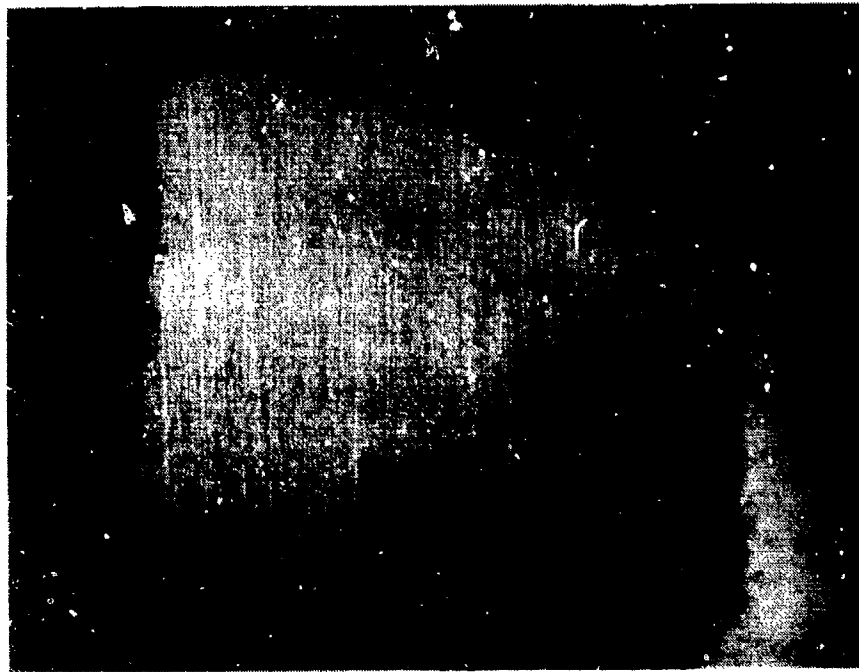
## MEASUREMENTS IN THE FUEL MIXTURE

A test cell was fabricated using a graphite counterelectrode and calomel standard reference and filled with the fuel mixture. A polished aluminum sample was inserted into the cell and immediately scanned. Figure 2 shows the initial measurement on this sample. This curve is quite typical. In particular, the intersection of the limiting slopes (linear region) of its cathodic and anodic branches, as the applied potential passes through 0, defines the metal's corrosion potential  $E_{corr}$ . This provides a value of corrosion current for the freely corroding metal, as indicated in Figure 2. Taken with physical information, this measured corrosion current can provide a value of uniform corrosion rate for the metal.

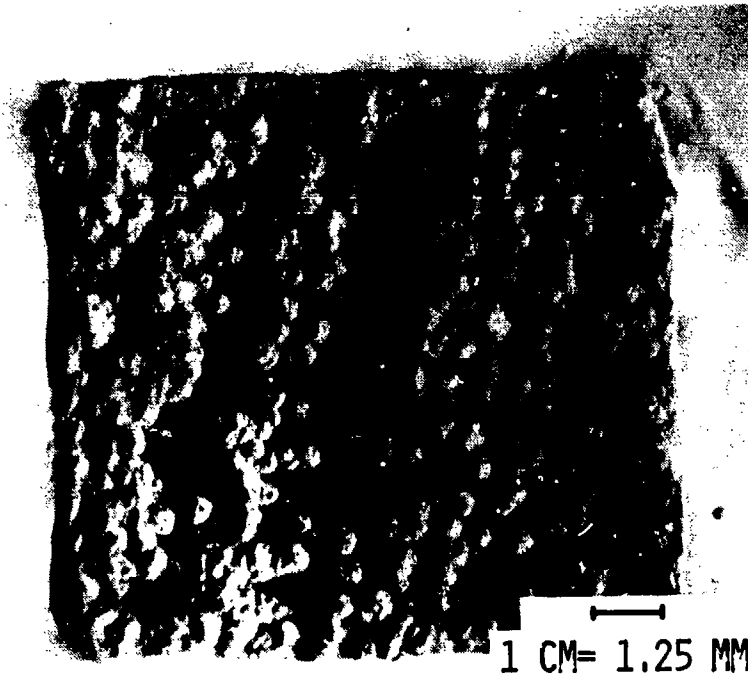
The anodic portion of the scan often will show a "passive" region (dotted addition in Figure 2), within which the current does not increase with increasing potential. This indicates a regime of surface protection, usually by an adherent oxide layer. Above this plateau, the protection breaks down and the corrosion current increases rapidly, often with the onset of pitting. In the present case, fairly wide ranging cathodic to anodic scan was employed. This was done specifically to place the test surface in a particularly corrosion vulnerable condition. If the "electrolyte" were to have a detrimental effect on the aluminum, such a scan would reveal it.

The corrosion rate as determined from the initial scan (Figure 2) was quite moderate [ $<1$  mil/year (mpy)]. The low measured corrosion current of  $1.6 \times 10^3$  nanoamps reflects the liquid's relatively low initial electrical conductivity. By way of comparison, an aluminum sample run in distilled water produced a corrosion current of  $0.5$ - $1.9 \times 10^2$  nanoamps. Typical corrosion currents observed in acidic electrolytes are several orders of magnitude larger. No anodic passivity was observed. Of particular concern, was the visible pitting almost immediately initiated on the anodic portion of the scan. A dark localized corrosion product emanated from the pits. Upon performing a second scan, it became evident that the pitting corrosion was extremely severe. The chemical action continued even after the potential was removed. This was the case despite a still relatively low calculated corrosion rate ( $\sim 2$  mpy). This finding points out the importance of visual observation to supplement the scans in a complete assessment of corrosion performance. Figure 3 shows the very severe pitting experienced by the aluminum during the pd scans. At this point, a serious incompatibility was obvious and further pd scans in the fuel mixture were suspended.

FIGURE 2. POTENTIODYNAMIC SCAN OF UNANODIZED 6061-T6 ALUMINUM IN FUEL MIXTURE CONTAINING CC1<sub>4</sub>



(BEFORE)



(AFTER)

FIGURE 3. SURFACE OF UNANODIZED 6061-T6 ALUMINUM BEFORE AND AFTER POTENTIODYNAMIC SCANS IN FUEL MIXTURE CONTAINING  $\text{CCl}_4$

### Theory of Pitting Corrosion

Since severe pitting immediately revealed itself the dominant corrosion process here, it seems appropriate to render a brief general discussion of the subject before seeking the particular mechanism at work in the solvent.

Pitting is a very localized corrosion attack which results in holes in a metal surface. It is perhaps the most destructive and insidious form of corrosion. These pits are often difficult to detect because of their small size and covering with corrosion products. As in the present case, the uniform corrosion appears minimal, but failures often occur with extreme suddenness.

The pitting mechanism can be considered an autocatalytic process. That is, the corrosion processes within the pit produce conditions which are both stimulating and necessary for continuing activity and propagation. This is illustrated schematically in Figure 4(upper). Here the Al metal, designated M, is being pitted by a chloride solution. Rapid dissolution occurs within the pit, while oxygen reduction takes place on adjacent surfaces. This activity is self-stimulating and self-propagating. This rapid dissolution of metal tends to produce an excess of positive charge in the area, resulting in the migration of chloride ions to maintain electroneutrality. Thus, in the pit, there is a high concentration of  $AlCl_3$  and, as a result of hydrolysis, a high concentration of hydrogen ions. Both hydrogen and chloride ions stimulate the dissolution of aluminum and the entire process accelerates with time. Since the solubility of oxygen is virtually zero in concentrated solutions, negligible oxygen reduction occurs within the pits. The cathodic oxygen reduction on the surfaces adjacent to the pits tends to suppress corrosion. In a sense, pits cathodically protect the rest of the metal surface.

### Application to Case of Aluminum in Fuel Mixture

The present case of aluminum exposed to a normally non-conducting organic solvent mixture presents a more unusual case of pitting reaction. The chloride "ions" are supplied by a unique type of anodic reaction. Examination of some standard corrosion texts revealed interesting information. Laque and Copson<sup>3</sup> make the following observations regarding the corrosion of aluminum alloys in halogenated hydrocarbons:

"Most halogenated hydrocarbons are compatible with aluminum alloys at ambient temperatures. Elevating the temperature to the boiling point may cause certain halogenated hydrocarbons to react with aluminum. Even under these conditions, however, compounds such as trichloroethylene and perchloroethylene are not reactive and have been successfully employed with aluminum for metal degreasing operations. Instances of unexpected corrosion by relatively inert halogen compounds (such as the above) have usually been traced to the

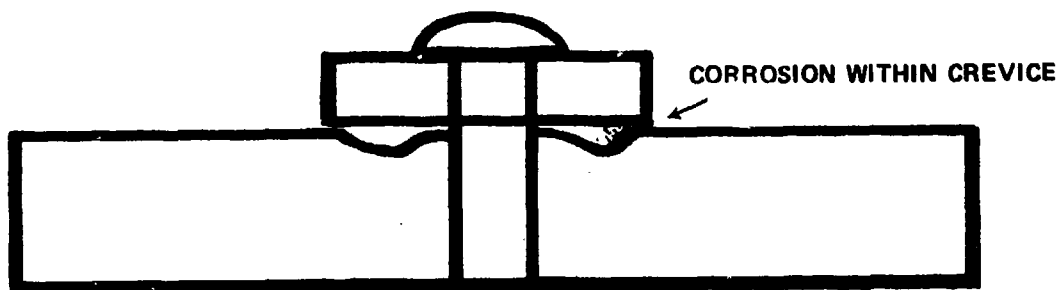
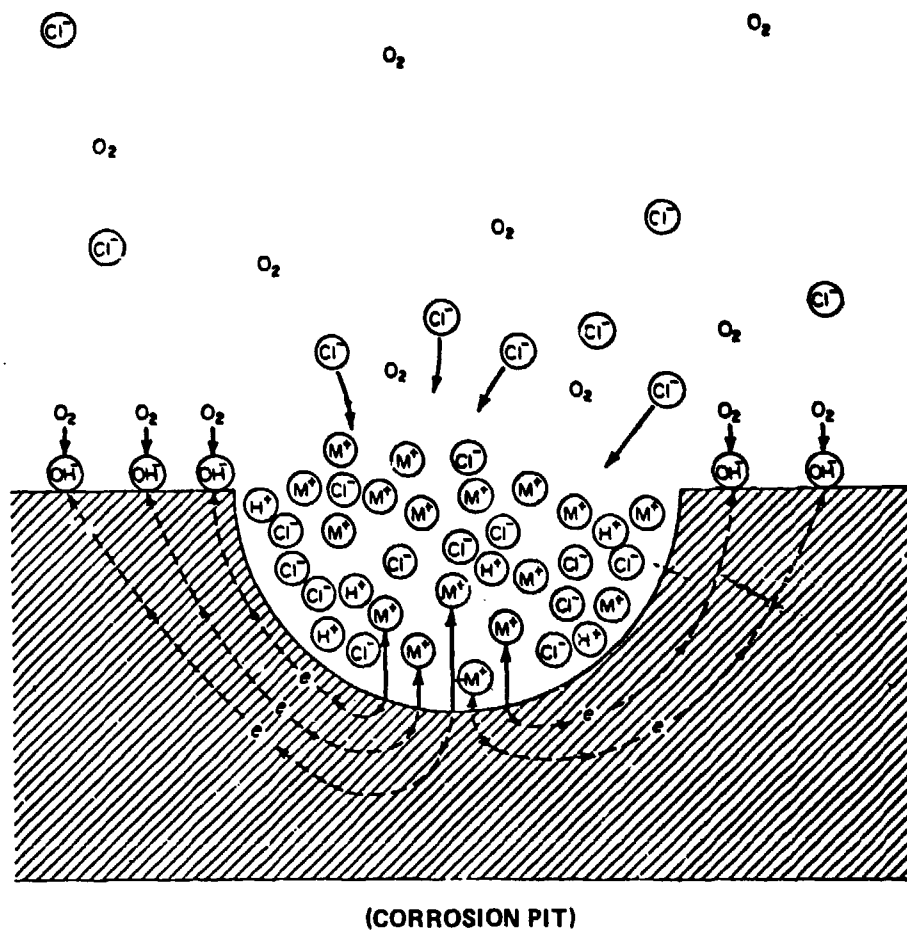


FIGURE 4. SCHEMATIC REPRESENTATIONS OF PITTING CORROSION AND CREVICE CORROSION

contaminant metals or other compounds which in turn have started a reaction with finely divided aluminum dust or chip... Other halogenated organic compounds which can be handled with aluminum are benzene hexachloride, benzoyl chloride, methyl chloride, vinyl chloride and dichloromonofluoromethane."

"The presence of moisture in halogenated hydrocarbons can lead to hydrolysis of the chloride to form hydrochloric acid which can attack aluminum. Precautions should be taken, therefore, to keep halogenated compounds as dry as possible."

"Aluminum reacts rapidly with boiling carbon tetrachloride to form aluminum chloride and hexachloroethane. A rather critical temperature dependence can be shown ranging from rapid reaction at the boiling point to negligible reaction in 18 months at room temperature. The presence of the reaction product aluminum chloride accelerates the reaction, whereas hexachloroethane has no effect. The aluminum chloride acts as an accelerator probably through the formation of complexes with the carbon tetrachloride."

The situation is made even more specific by Uhlig:<sup>4</sup> "Severe accidents have been caused by the high reaction rate of aluminum with anhydrous chlorinated solvents such as in the degreasing of castings, ball milling of Al flake with  $\text{CCl}_4$ , or even in the case of Al used as a container at room temperature for mixed chlorinated solvents. The reaction with  $\text{CCl}_4$ , for example has been shown to follow:



the hexachloroethane ( $\text{C}_2\text{Cl}_6$ ) is given up, while the  $\text{AlCl}_3$  remains in the pit vicinity as an autocatalyst. The corrosion rate for 99.99% Al in boiling anhydrous  $\text{CCl}_4$  is very high, e.g., 37,500 mdd (20,000 mils/yr). Should the temperature reach the melting point of aluminum, the reaction may proceed explosively. An induction time in the order of 55 minutes, during which corrosion is negligible, precedes the rapid rate. This induction time is lengthened either by the presence of water in the  $\text{CCl}_4$  (480 min) or by some alloying additions, e.g., Mn or Mg (30 hours for type 5052). On the other hand, addition of  $\text{AlCl}_3$  or  $\text{FeCl}_3$  to  $\text{CCl}_4$  decreases the induction time to zero without appreciable effect on the induction rate. The corrosion rate of Al in water-saturated  $\text{CCl}_4$ , following a prolonged induction time, is about twice that in the anhydrous solvent."

A corrosion reactivity of this severity would pierce the 125 mil aluminum vessel wall within a few days storage at the specified maximum temperature of 160°F after pit initiation. This reaction is especially insidious because of its exothermal nature. The emitted heat raises the local temperature, which, in turn, further abets the reaction.

## MEASUREMENTS IN PURE METHANOL

Having encountered the severe incompatibility with the solvent fuel mixture, attention was focused on pure methanol as an alternative. The method of pd scanning again was employed to obtain timely corrosion compatibility information.

Mounted samples of each metal surface of Table 1 were prepared as previously described. A new test cell containing graphite counter and standard calomel reference electrode was fabricated. Since numerous pd scans were run in this series, care was taken that the electrolyte not become contaminated. In particular, there had been some concern of possible contamination of the methanol electrolyte by the gradual infiltration of chloride ions from the KCl solution contained in the reference electrode. Periodic chemical checks were made for this condition by introducing  $\text{AgNO}_3$  solution into small samples of the used electrolyte. Fortunately, no chloride ions were detected at any time. The standard calomel electrode, therefore, should be suitable for future studies with organic electrolytes of this type. It is to be noted that the methanol electrolyte used in this cell was in continuous contact with the atmosphere and, therefore, is presumed to contain the equilibrium content of absorbed water (~0.5%).

Again the potentiodynamic scans were taken over a wide cathodic to anodic range in order to be certain of revealing any incipient pitting, etc. A PARC 351 corrosion measurement system was used to obtain the scans, which were recorded for possible further analysis at a later date. Another goal of these measurements was to observe any significant increase over time of the uniform corrosion rate, which might lead to premature device failure. An initial scan was taken in each case as soon as possible after immersion. Each sample then was left immersed at ambient temperature for 24 hours in the fuel and another scan taken (some with intermediate scans). All pd scans were carried out at ambient temperature.

Figures 5, 6 and 7 contain photographs taken before and after the pd scan series in pure methanol, respectively, of the anodized aluminum cavity wall, steel nose section and unanodized aluminum samples. The rough white material visible around the sample perimeter is epoxy masking paint. Representative pd scans are given in Figures 8 and 9. The Parcalc fit data on the scans refers to a built in calculation which produces a weighted fit to the important linear (Tafel) region of the potential versus current curve around  $E_{\text{corr}}$  based on corrosion theory. Agreement with manual estimation of the Tafel slopes was fair. To avoid confusion, only the manual measurements of  $I_{\text{corr}}$  and corrosion rates are included in the data of Table 2. The post-scan pictures of Figures 5 and 6 show no evidence of pitting.

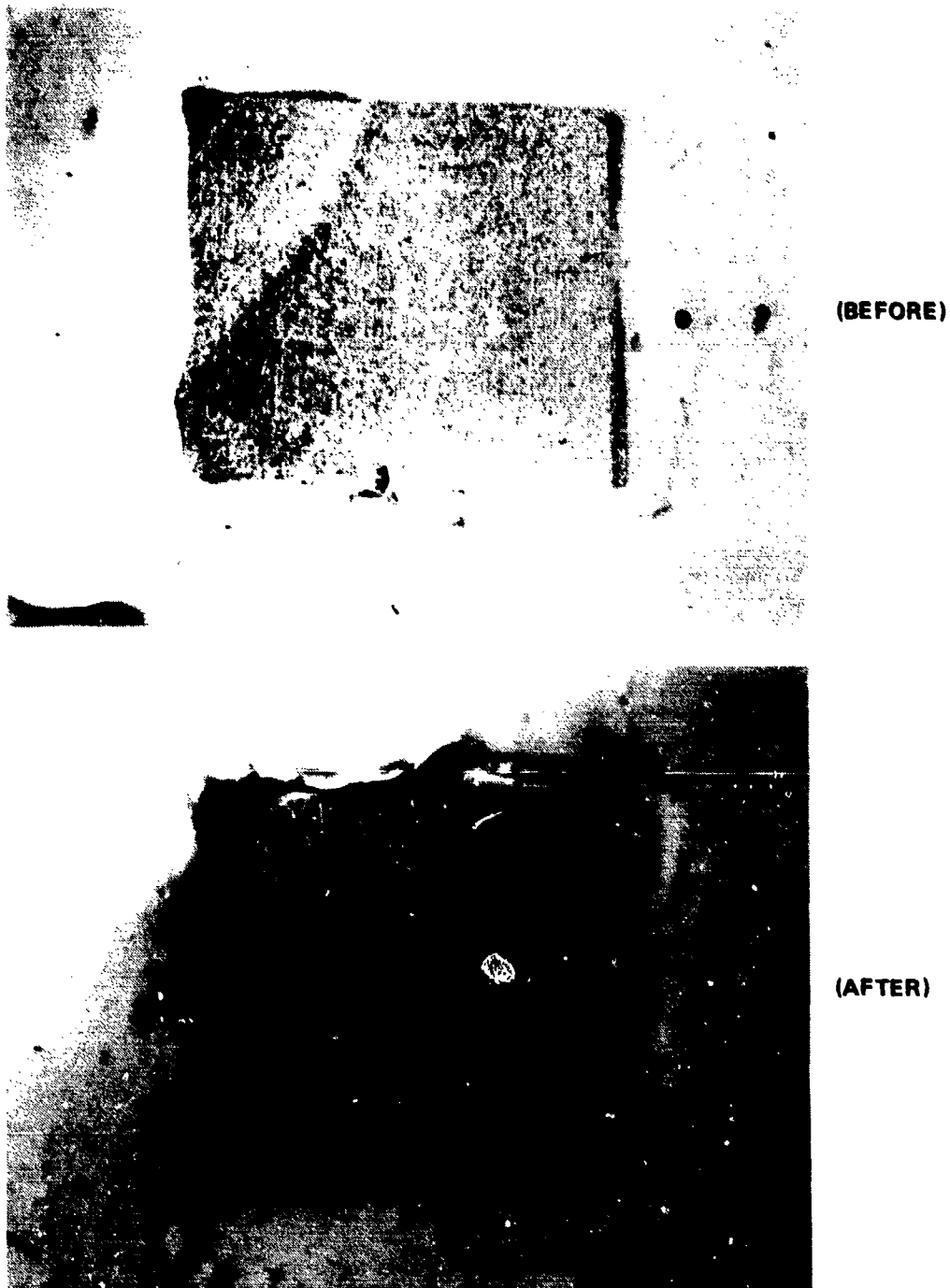
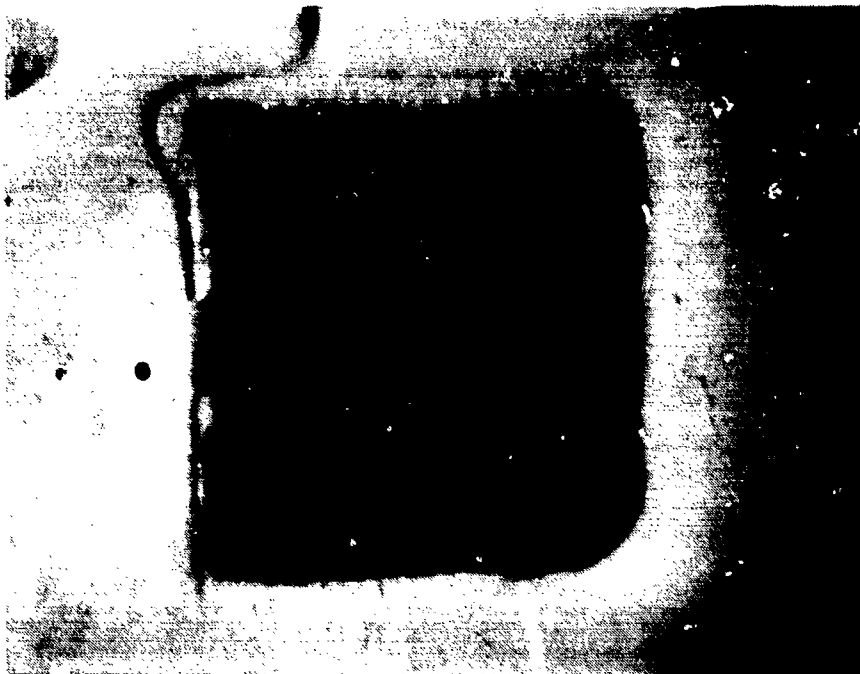


**FIGURE 5. ANODIZED 6061-T6 ALUMINUM SURFACE BEFORE AND AFTER POTENTIODYNAMIC SCANS AND 24 HOUR IMMERSION IN METHANOL**



(BEFORE)

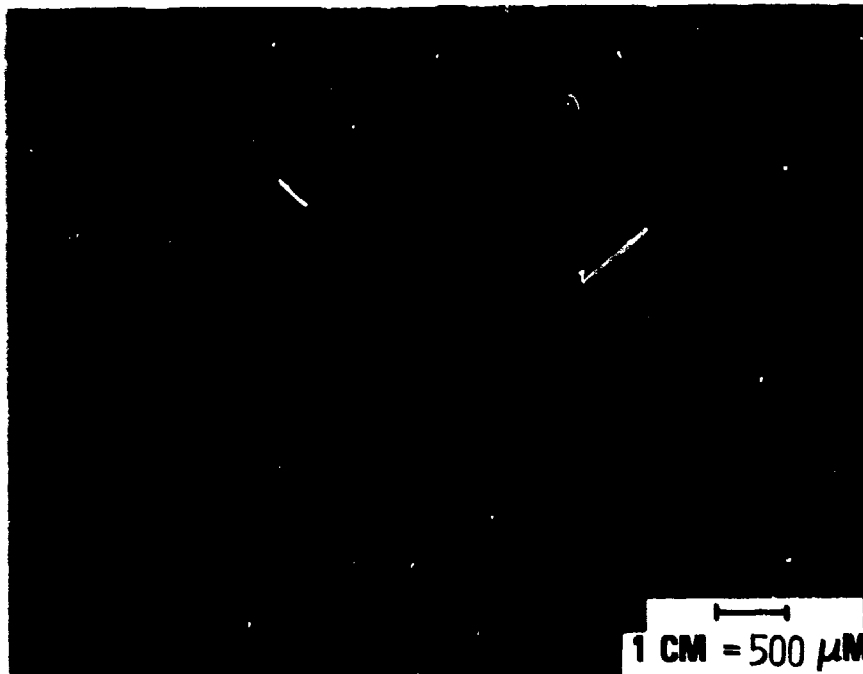


(AFTER)

**FIGURE 6. ZINC-PLATED STEEL SURFACE BEFORE AND AFTER POTENTIODYNAMIC SCANS AND 24 HOUR IMMERSION IN METHANOL**



(BEFORE)

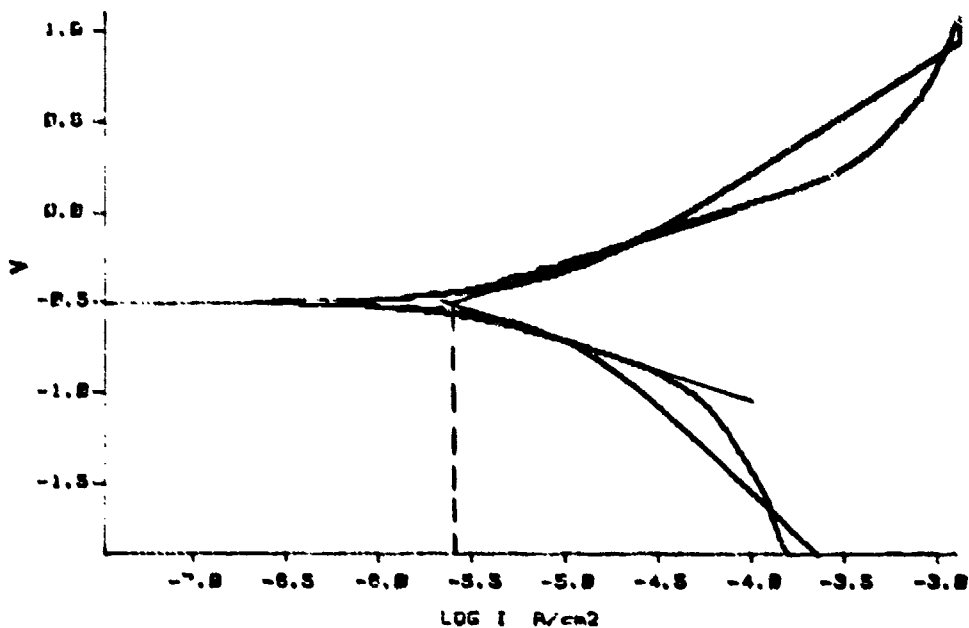


(AFTER)

1 CM = 500  $\mu$ M

FIGURE 7. UNANODIZED 6061-T6 ALUMINUM SURFACE BEFORE AND AFTER POTENTIODYNAMIC SCANS AND 24 HOUR IMMERSION IN METHANOL

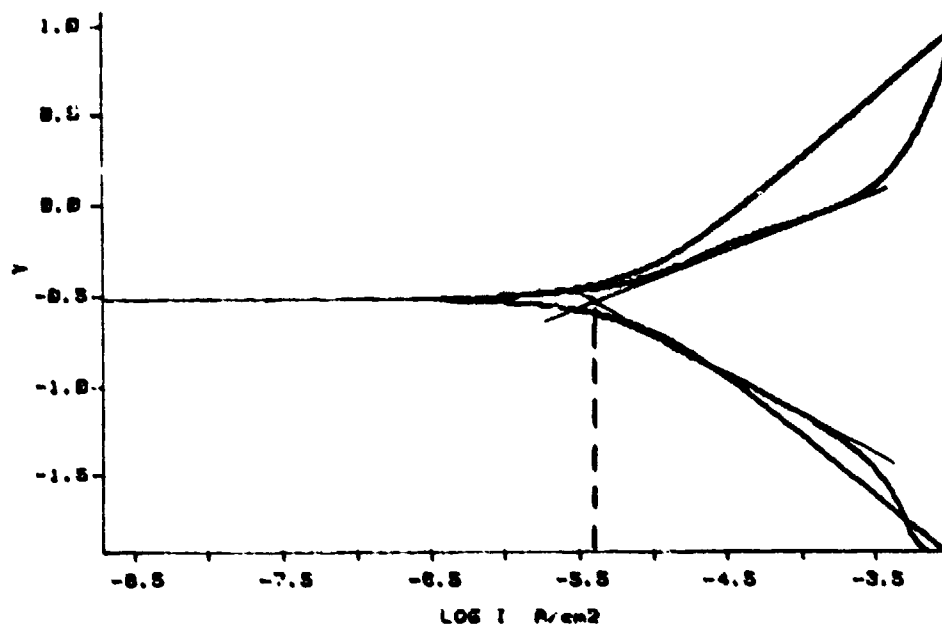
MODEL 351 CORROSION MEASUREMENT SYSTEM	ALUAMETH 21 OCT 1986
COMMENT: 6061-T6 UNAN 3 MIN	



POTENTIODYNAMIC					
DATE CREATED	21	OCT	1986	RUN DATE	21 OCT 1986
IR COMP	=	DISABLED		TAFEL BETA a	= 0.662 V/DEC
FINAL E	=	1.0 V ~ Ec		TAFEL BETA c	= 0.977 V/DEC
INITIAL E	=	-1.2 V ~ Ec		Ecorr	= -0.690 V
INITIAL DELAY	=	60 SEC		E(I=0)	= -0.496 V
SCAN RATE	=	2 mV/SEC		Icorr	= 8 E-6 A/cm²
				CORR RATE	= 4 ED MPY
				(Parcalc)	
EQUIV WEIGHT	=	9 g/EQUIV		Icorr	= 2.5 E-6
DENSITY	=	2.7 g/cm³		CORR RATE	= 1.25 MPY
AREA	=	1 cm²			(Direct measurement)

FIGURE 8. POTENTIODYNAMIC SCAN OF UNANODIZED 6061-T6 ALUMINUM IN METHANOL

MODEL 351 CORROSION MEASUREMENT SYSTEM	FEZNMETH 22 OCT 1986
COMMENT: STEEL 1010-20 ZN PL 3 MIN	



POTENTIODYNAMIC					
DATE CREATED	22	OCT	1986	RUN DATE	22 OCT 1986
IR COMP	=	DISABLED			
FINAL E	=	1.0 V ~ Ec			
INITIAL E	=	-1.2 V ~ Ec			
INITIAL DELAY	=	60 SEC			
SCAN RATE	=	2 mV/SEC			
EQUIV WEIGHT	=	27.9 g/EQUIV			
DENSITY	=	7.8 g/cm3			
AREA	=	1 cm2			
				TAFEL BETA a	= 0.693 V/DEC
				TAFEL BETA c	= 0.671 V/DEC
				Ecorr	= -0.729 V
				E(I=0)	= -0.515 V
				Icorr	= 7 E-6 A/cm2
				CORR RATE	= 3 ED MPY
				(Parcalc)	
				Icorr	= 4.5 E-6
				CORR RATE	= 1.93 MPY
				(Direct measurement)	

FIGURE 9. POTENTIODYNAMIC SCAN OF ZINC-PLATED STEEL IN METHANOL

TABLE 2. CORROSION DATA ON TESTED METALS IN PURE METHANOL  
BY POTENTIODYNAMIC SCANNING

MATERIAL	IMMERSION TIME	(mpy)	I <sub>corr</sub> (μA)	E <sub>corr</sub> *
6061-T6 Al ANODIZED	3 min	0.004	0.01	-0.77
	6 hrs	0.28	0.63	-0.87
	24 hrs	0.18	0.4	-0.8
6061-T6 Al UNANODIZED	3 min	1.3	2.5	-0.7
	24 hrs	3.2	6.3	-0.82
1010-20 STL Zn PLATED	3 min	1.9	4.5	-0.73
	24 hrs	10.0	23.4	-0.72
5052-32 Al ANODIZED SCREEN	10 min	0.6	1	-0.75
	24 hrs	0.14	0.32	-0.54

\* REFERENCED to STANDARD CALOMEL ELECTRODE

The corrosion rates of Table 2 calculated from the scans of the anodized aluminum and steel samples are relatively modest with some indication of greater corrosion of the steel. In the case of the anodized Al surface (Figure 5), Table 2 shows an initial rise in corrosion rate from 0.004 to 0.28 mpy followed by a decline to 0.18 mpy at 24 hours immersion. This indicates the tendency of this surface toward passivation in the methanol. This is a desirable condition, as the corrosion rate likely will settle to a comfortably low value. The steel sample of Figure 6(bottom) shows evidence of some zinc plating removal, but is otherwise unaffected.

The polished, unanodized aluminum sample of Figure 7 shows a somewhat different behavior under potentiodynamic scanning. Table 2 indicates a corrosion rate of 1.3 mpy on the initial scan. After 24 hours immersion and a second scan, the computed corrosion rate had increased to 3.2 mpy. Thus, in the absence of the protective oxide layer, early passivation is not established. A longer term experiment would be necessary to determine the extent of eventual passivation in the methanol. Here the presence of absorbed water may play a critical role. Generally, aluminum alloys will passivate in pure water. However, if sufficient water is not present to help stabilize and replenish the oxide layer, passivation may not be maintained even in a relatively nonhostile environment such as methanol.

Although the corrosion rate of this unanodized sample is some 10X that of the anodized surface, it is still at an acceptable level, provided passivation eventually is established. Of perhaps greater concern is the rather fine scale incipient pitting evident after the 2 scans and 24 hour immersion [Figure 7(bottom)]. These pits are apparently slow-growing. They probably result from a general inadequacy of the initial oxide layer on the aluminum surface coupled with the lack of sufficient oxygen, rather than any great hostility of the electrolyte medium. Nevertheless, the relative dearth of available oxygen for protective oxide layer healing could allow the conditions for serious pitting to develop. This all points to the value of the anodization in preventing initial deterioration of the oxide layer.

## CHAPTER 4

## PART II: GALVANIC CORROSION

## BACKGROUND

Since the dissimilar metals aluminum and steel are present in contact in the fuel wetted portion of the device, a galvanic couple will be set up with the fuel as electrolyte. Table 3 gives the galvanic series of many important metals in seawater. Generally, metals located close to one another in this series do not experience serious galvanic effects. While the predictions of this table are not directly applicable to other electrolytes, large galvanic currents still are unanticipated with this couple-liquid combination. The system, however, must be tested to be certain of complete compatibility.

## EXPERIMENTAL

Samples were cut from actual surface treated portions of the steel nose and aluminum body. These were cold mounted with electrical wire connections. The samples were masked to achieve approximately the fuel wetted area ratio of steel to aluminum found in the device (about 1:20.6). The photograph (Figure 10) shows the mounted samples before the galvanic couple corrosion test in methanol. Enlarged photographs of the surfaces were taken for later comparison. The samples subsequently were mounted in a cell of one liter capacity. A standard calomel electrode was used as reference. The PARC 351 Corrosion Measurement Console was used in its galvanic couple mode to monitor the galvanic current and corrosion potential over a period of about six weeks. The measurements were made frequently during this period. During the entire period the immersed samples were electrically connected. The corrosion cell was exposed to the air during the entire period, allowing equilibrium quantities of water vapor and oxygen to be absorbed into the electrolyte. Additional methanol was added regularly due to evaporation.

TABLE 3. GALVANIC SERIES IN SEAWATER FOR VARIOUS METALS

Cathodic  
(Most Noble)



Anodic  
(Active)

Platinum  
Gold  
Graphite  
Titanium  
Silver  
Zirconium  
Type 316, 317 Stainless Steel (passive)  
Type 304 Stainless Steel (passive)  
Type 410 Stainless Steel (passive)  
Nickel (passive)  
Silver Solder  
Cupro Nickels (70-30)  
Bronzes  
Copper  
Brasses  
Nickel (active)  
Naval Brass  
Tin  
Lead  
Type 316, 317 Stainless Steels (active)  
Type 304 Stainless Steel (active)  
Cast Iron  
Steel or Iron  
Aluminum 2024  
Cadmium  
Aluminum (commercially pure)  
Zinc  
Magnesium and Magnesium Alloys

(From: "Zircadyne<sup>Tm</sup> Corrosion Data" Publication by Teledyne  
Wah Chang, Albany, OR 97321)

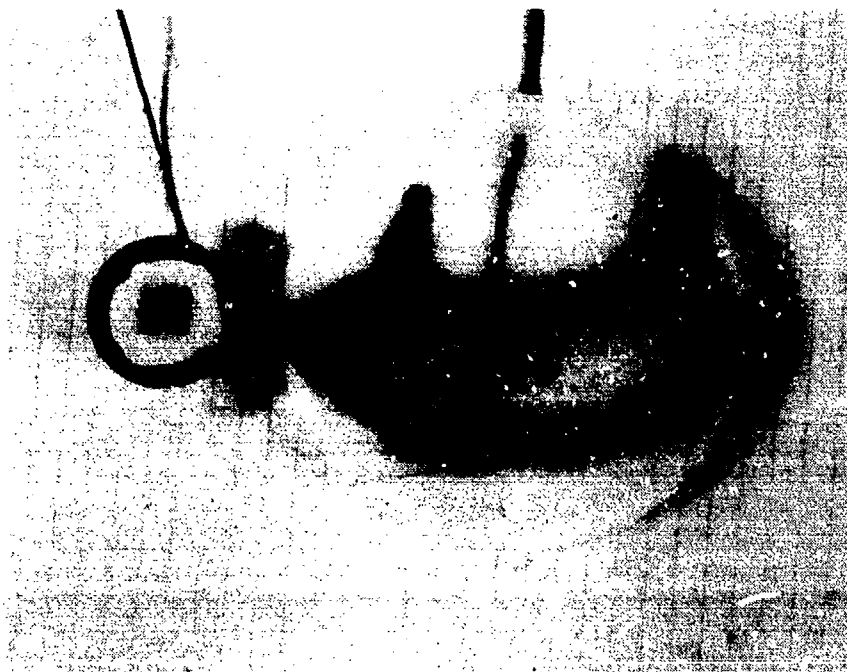


**FIGURE 10. COLD-MOUNTED ZINC-PLATED STEEL AND ANODIZED 6061-T6 ALUMINUM SAMPLES IN THE TRUE FUEL WETTED AREA RATIO, BEFORE GALVANIC CORROSION TEST**

## RESULTS

Figure 11 is an output scan of current versus time for the couple taken on the Corrosion Console. Such monitoring scans were made frequently during the test. The average current was extracted from each scan and used to plot Figure 12. Figure 12 shows the galvanic current in nanoamps/cm<sup>2</sup> versus time in hours over the entire test period. The cell was connected to the measurement instrument with polarity assuming the aluminum electrode to be anodic. Thus the designation on the current axis refers to this electrode. The results show that, through about the first 400 hours, the aluminum was actually cathodic. The steel, therefore, was the corroding (anodic) member during this period. This was not unexpected, however, since the zinc plating should act as a sacrificial electrode. After the zinc has dissolved, the galvanic current may be expected to reverse.

The aluminum becomes anodic. The galvanic current subsequently continues to increase, saturating at 1-1.2 microamps/cm<sup>2</sup> after about 1000 hours exposure. The saturating behavior indicates the possible gradual formation of a partially protective thick oxide layer on the aluminum. Figure 13 shows the corrosion potential  $E_{corr}$  versus time. The sign change at 400 hours and limiting negative trend toward the conclusion of the test confirm the conclusions above. The apparent instability of  $E_{corr}$  at this point might indicate some breakdown or defects in the developed protective oxide film. By way of comparison, Figure 14 shows the same galvanic couple in a 3.5% NaCl electrolyte.\* The corrosion current density is some 15-20X larger in this case. It is shown below that even this rate of corrosion is not serious, provided significant pitting is not occurring.

Figure 15 shows the mounted steel sample before (top) and after (bottom) the test. The masking paint has been removed from the post test sample, revealing the cut sample edges. Although corrosion activity has taken place beneath the masked portion, the arrows point out small sections of zinc plating remaining. The removal of the zinc, therefore, from the exposed surface correlates with the change in polarity of the galvanic corrosion current at 400 hours (Figure 12).

The measurements of Figure 12 indicate a saturating galvanic current of 1.0 to 1.2 microamps/cm<sup>2</sup> at the aluminum member which is the predominant corroding (anodic) component after dissolution of the zinc plating on the steel. Computation of the corresponding corrosion rate in milli-inches/year (mpy) is as follows:

Where: EW= equivalent weight

d= density

mpy=  $\{EW \cdot I_{corr} / d \cdot F \cdot A\} \cdot 1.26 \cdot 10^4$

F= 96,500 Coulombs (Faraday)

A= Sample area

\*Data courtesy of Dr. Jack McIntyre (R33), NSWC Corrosion Group

MODEL 351 CORROSION MEASUREMENT SYSTEM	<b>ALSTMETH</b> 9 JUN 1987
COMMENT: AL-STEEL COUPLE F26 PROPORTIONAL AREAS	



GALVANIC CORROSION			
DATE CREATED	9 JUN 1987	RUN DATE	9 JUN 1987
RUN TIME	= 3600 SEC		
EQUIV WEIGHT	= 9 g/EQUIV	E <sub>corr</sub>	= -0.1 V
DENSITY	= 2.81 g/cm <sup>3</sup>	E[ <i>I</i> =0]	= 0 V
AREA	= 20.6 cm <sup>2</sup>		

FIGURE 11. ALUMINUM-STEEL GALVANIC COUPLE CORROSION SCAN: GALVANIC CURRENT VERSUS TIME IN METHANOL

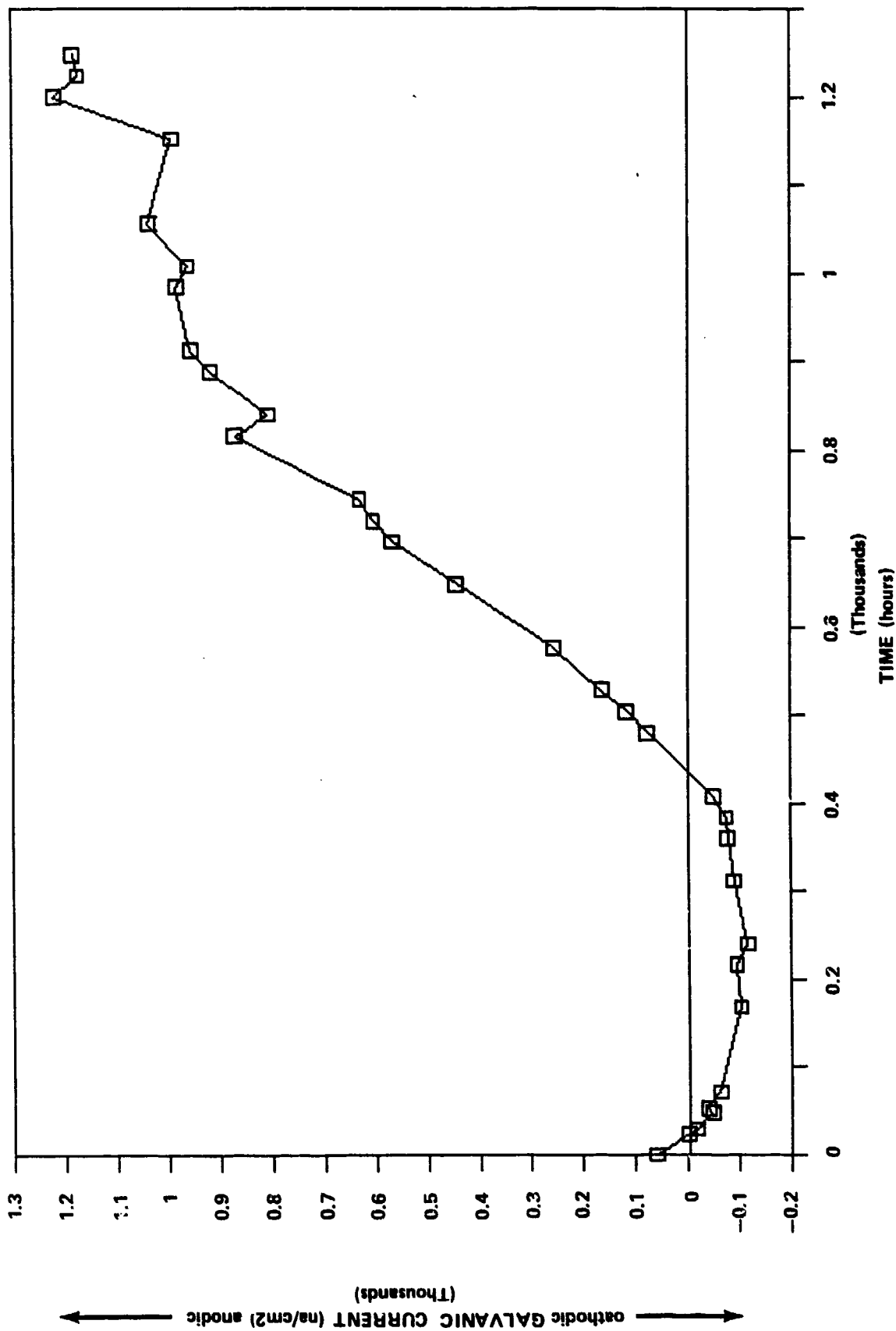


FIGURE 12. GALVANIC CURRENT DENSITY VERSUS TIME FOR ZINC-PLATED STEEL/6061-T6 ALUMINUM COUPLE IN METHANOL

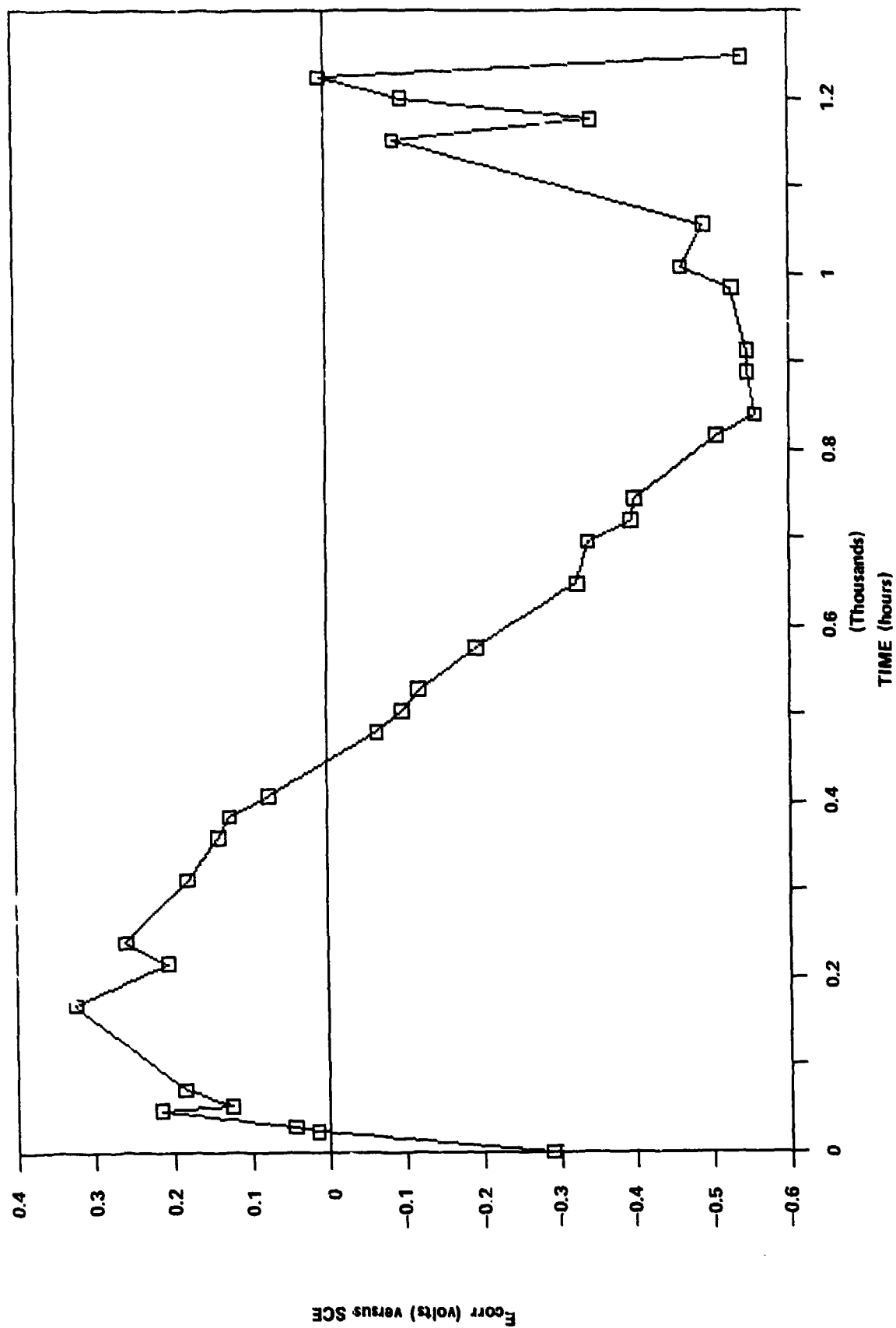


FIGURE 13. CORROSION POTENTIAL  $E_{corr}$  VERSUS TIME FOR ZINC-PLATED STEEL/6061-T6 ALUMINUM COUPLE IN METHANOL

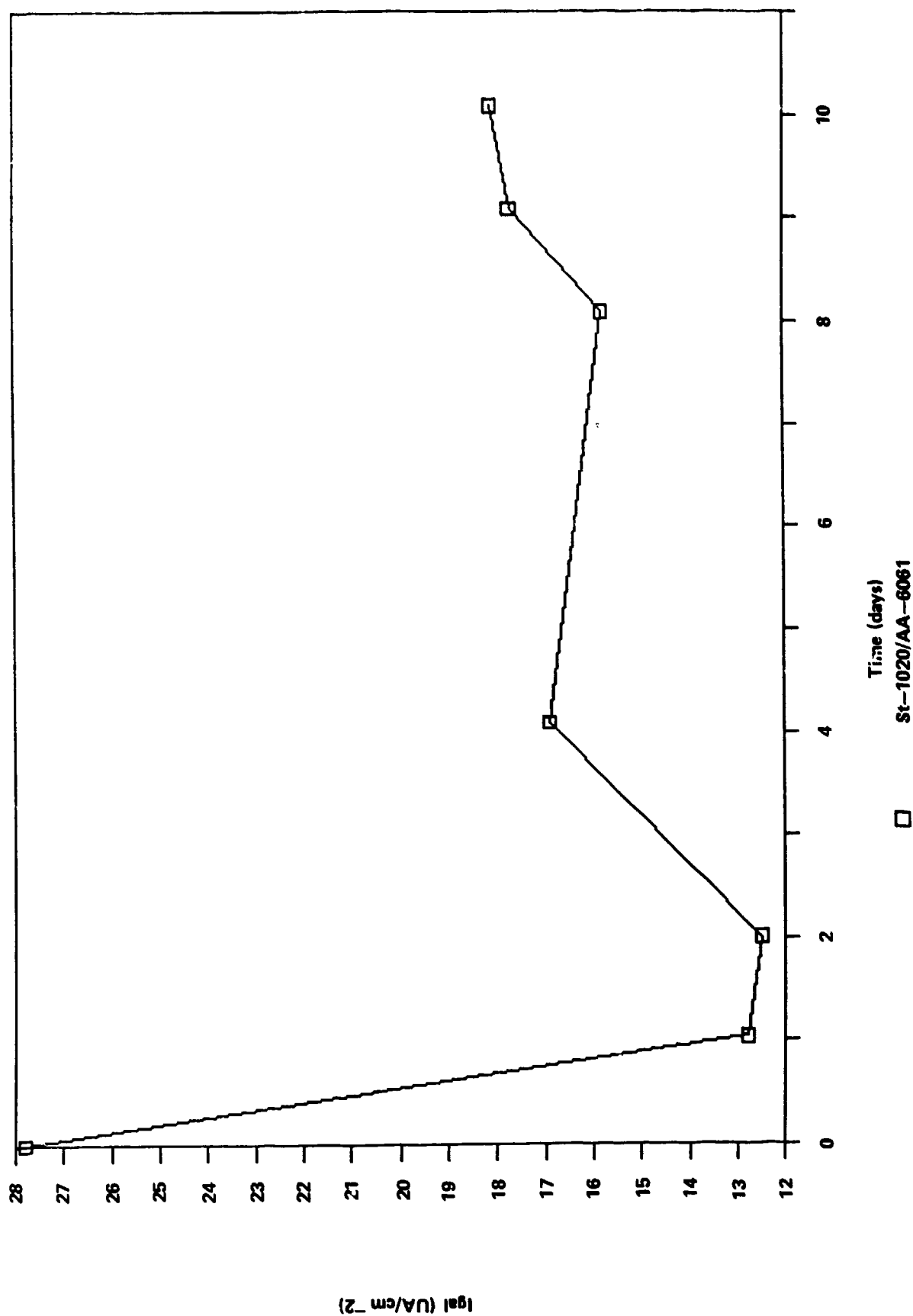
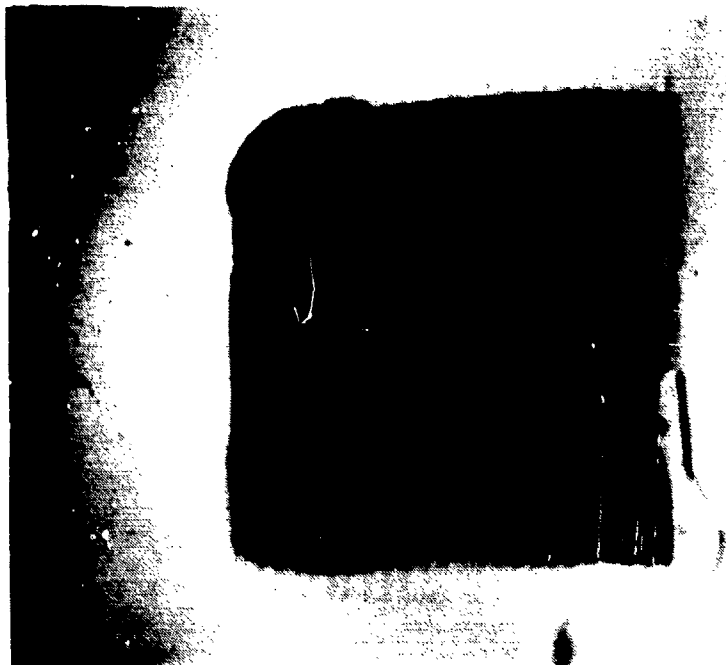
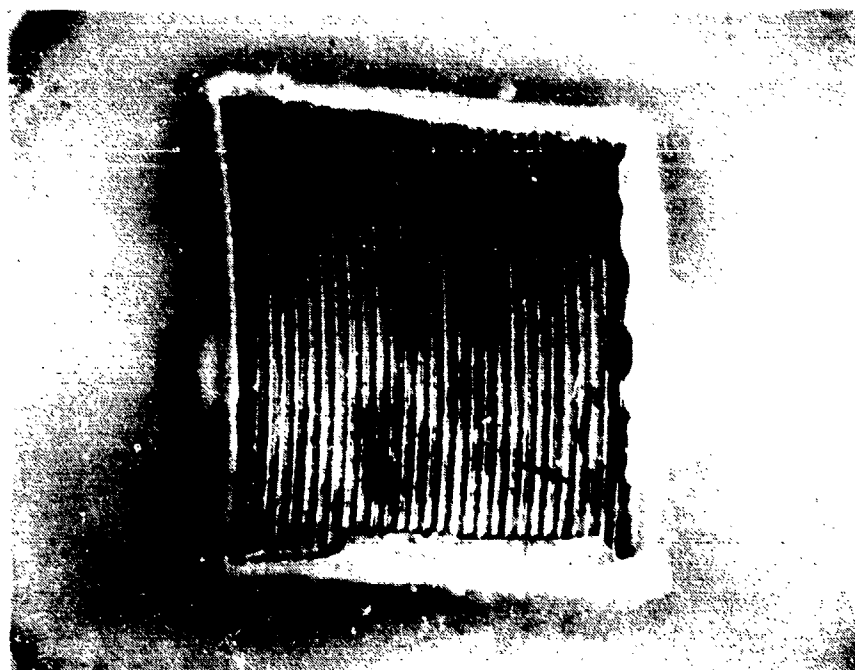


FIGURE 14. GALVANIC CURRENT DENSITY VERSUS TIME FOR 1020 STEEL/6061-T6 ALUMINUM COUPLE IN 3.5% NaCl SOLUTION



(BEFORE)

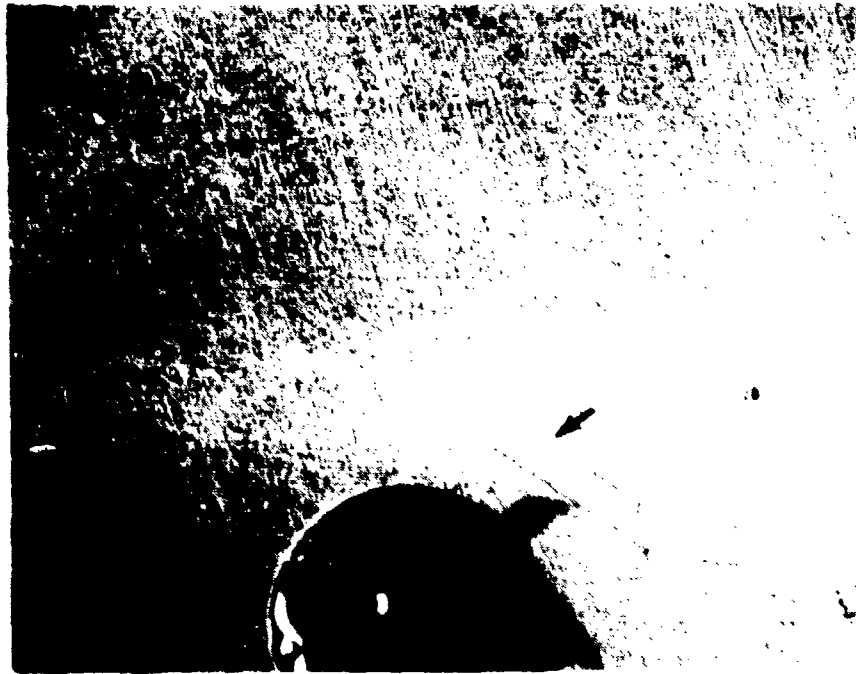


(AFTER)

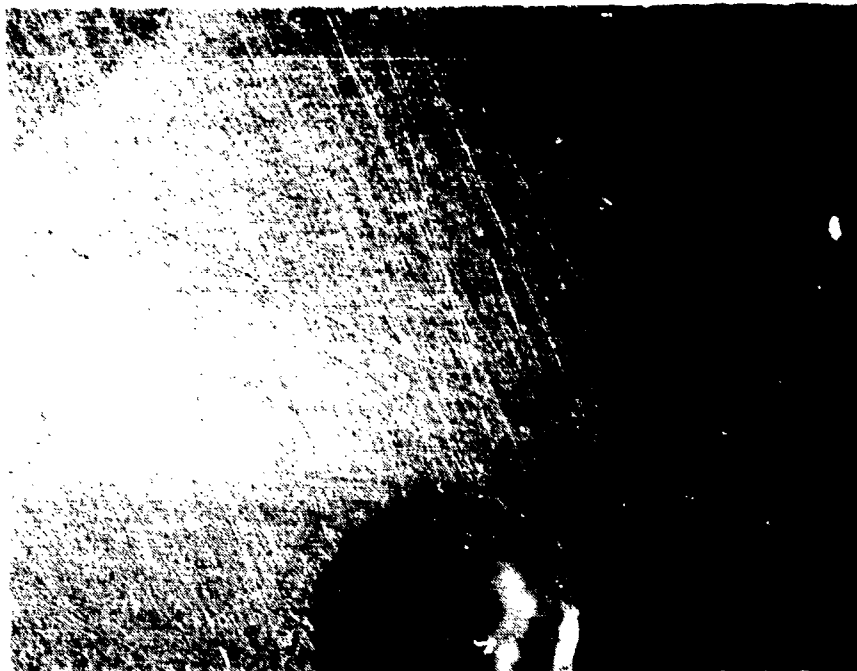
**FIGURE 15. ZINC-PLATED STEEL SURFACE BEFORE AND AFTER GALVANIC CORROSION TEST IN METHANOL**

Applying the above to the aluminum with the observed current range results in a negligible corrosion rate of  $0.5-0.6 \times 10^{-6}$  mpy. This corrosion rate might change somewhat had the test progressed further, however, experience has shown that further significant changes will not occur.

Probably more importantly, the couple was examined for evidence of pitting at the test termination. Figure 15 indicates no pitting of the steel electrode. Figure 16 shows the same enlarged surface area of the aluminum electrode before (top) and after (bottom) the test. Detailed examination indicates no pitting. Even scratches remain virtually identical in appearance after the test. Pitting, therefore, as a component of the galvanic corrosion of the metals in methanol does not seem to be a problem.



(BEFORE)



(AFTER)

**FIGURE 16. ANODIZED 6061-T6 ALUMINUM SURFACE BEFORE AND AFTER GALVANIC CORROSION TEST IN METHANOL**

## CHAPTER 5

## PART III: CREVICE CORROSION

## BACKGROUND

The O-ring groove area constitutes a crevice which may trap and concentrate stagnant corrosive compounds from the electrolyte. This is shown schematically in Figure 4(lower). These compounds could preferentially corrode the groove area, causing leaks in the system. An elevated temperature test was designed and carried out to examine this possibility. At the same time, some information accrued on compatibility of the O-ring material itself. This information is necessarily qualitative and limited in scope to compatibility of the given test material. Such data is actually incidental to a corrosion test, but has been included in this section because of its important consequences in the device involved.

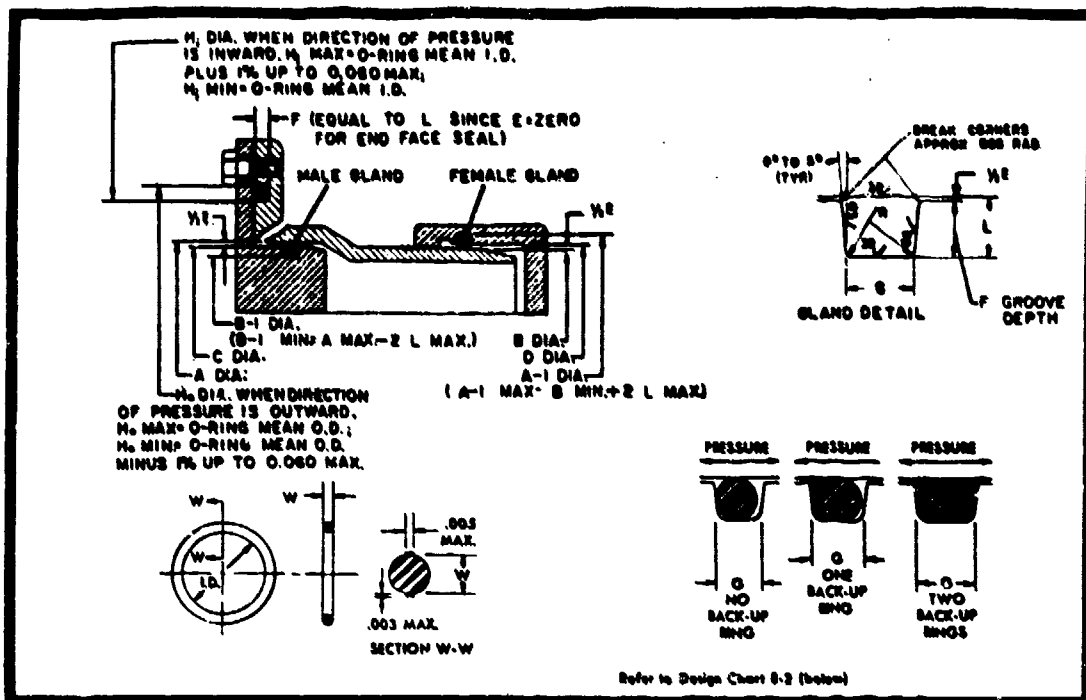
## EXPERIMENTAL

Four small vessels about 3 inches in length, consisting of 6061-T6 aluminum canisters about 3 inches long were fabricated with mating steel 1018 caps. The cans and caps were sized to fit with proper O-ring tolerance. Likewise, the O-ring groove was machined into the steel cap according to the specifications for the given O-ring found in Figure 17. The tops were made with four threaded holes above the groove for holding them firmly in place with small screws, against the internal pressure of some 15 lbs/in<sup>2</sup> at 70°C. This configuration reproduces the device fuel chamber, in scale, with reasonable accuracy. The O-ring size was that used between fuel chamber and gas generator in the actual device.

In order to extract the maximum corrosion information possible, subject to the limited number of samples, the containers were organized into a small test matrix (a larger number of samples usually are tested, as corrosion tests are by nature statistical). Two container sets were anodized/Zn plated according to specifications\*,\*\* for the aluminum and steel parts, respectively. Photo-

\*Aluminum anodized in accordance with MIL-A-8625, Type II, Class I.

\*\*Zinc plate in accordance with ASTM B633-78, Class Fe/Zn 13, SC3, Type II.



(A) INDUSTRIAL O-RING SEAL GLANDS

O-Ring Size Part 2-	W Cross Section		L Gland Depth	Squeeze		E (m) (c) Diametrical Clearance	G Groove Width			R Groove Radius	Eccentricity Max. (in)
	Nominal	Actual		Actual	%		No Back-Up Rings	One Back-Up Ring	Two Back-Up Rings		
004 through 050	$\frac{1}{16}$	.070 ±.003	.050 to .052	.015 to .023	22 to 32	.002 to .005	.093 to .098	.138 to .143	.205 to .210	.005 to .015	.002
102 through 178	$\frac{1}{8}$	.103 ±.003	.081 to .083	.017 to .025	17 to 24	.002 to .005	.140 to .145	.171 to .176	.238 to .243	.005 to .015	.002
201 through 284	$\frac{3}{16}$	.139 ±.004	.111 to .113	.022 to .032	16 to 23	.003 to .006	.187 to .192	.208 to .213	.275 to .280	.010 to .025	.003
309 through 395	$\frac{1}{2}$	.210 ±.005	.179 to .173	.032 to .045	15 to 21	.003 to .006	.281 to .286	.311 to .316	.410 to .415	.020 to .035	.004
425 through 475	$\frac{5}{8}$	.275 ±.006	.226 to .229	.040 to .055	15 to 20	.004 to .007	.375 to .380	.408 to .413	.538 to .543	.020 to .035	.005

(B) DESIGN CHART

FIGURE 17. DESIGN CHART FOR INDUSTRIAL O-RING STATIC SEAL GLANDS

graphs of the test container O-ring groove areas were taken before filling. The surfaces of the remaining two vessels were intentionally left untreated. Figure 18 shows a pair of these vessels. The difference in appearance of the surface treated container on the left may be noted.

Figure 19(top) is a close view of the O-ring groove vicinity in the plated steel cap before filling and closure. Figure 20(top), likewise, is a view of the O-ring contacting portion of the cylindrical aluminum vessel wall. A broad in focus area is not easily attainable here because of the geometry. The O-rings were lightly greased with the compound normally used in the device.

Two vessels, one with and one without treated surfaces, were placed in a glove box, prepared for this purpose. These vessels were filled with methanol after evacuating and backfilling 3 times with argon (Ar) gas. The methanol itself was neither de-aerated nor dried. The remaining two vessels were filled in air. The fluid level was adjusted to about 0.5-1 cm below the O-ring with the caps inserted. After fitting the steel caps using the retaining screws, the vessels were sealed in glass bottles. These bottles were placed horizontally in a controlled temperature water bath at 70°C (160°F). After two days, the bottles were removed to check for water leaks. At this point, the bottles were resealed with rubber top gaskets after weighing each test vessel. These weights provided a reference to determine leakage of the fuel from the vessels over the 3 month test period.

The intent of the test matrix was to discover the effect of trapped air above the fluid versus an inert gas. Simultaneously, the untreated vessels were intended to track the possible progression of crevice corrosion after dissolution of the anodization/zinc plating films. It must be recalled, however, that any corrosion normally will be limited in a sealed vessel by the residual free and dissolved oxygen, except in the case of corrosion promoting decomposition of the electrolyte itself as occurred with the fuel mixture containing  $\text{CCl}_4$ . This test has examined and eliminated this possibility for pure methanol. The containers were placed horizontally during the test, since this will be the normal position of the devices during storage.

#### ISSUES CONCERNING THE SEALED CAVITY CORROSION TEST

1. The progression of crevice corrosion (if any) at the O-ring groove in methanol:
  - a. The effect of trapped oxygen
  - b. Assessment of the effectiveness of surface treatments (e.g., anodizing and zinc plating)
  - c. Possible breakdown of fuel under long term de-aerated conditions

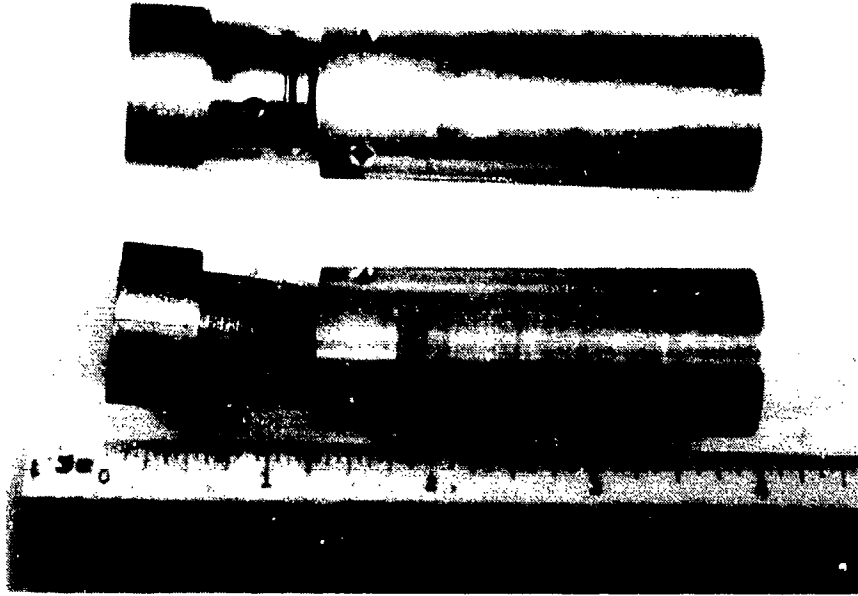
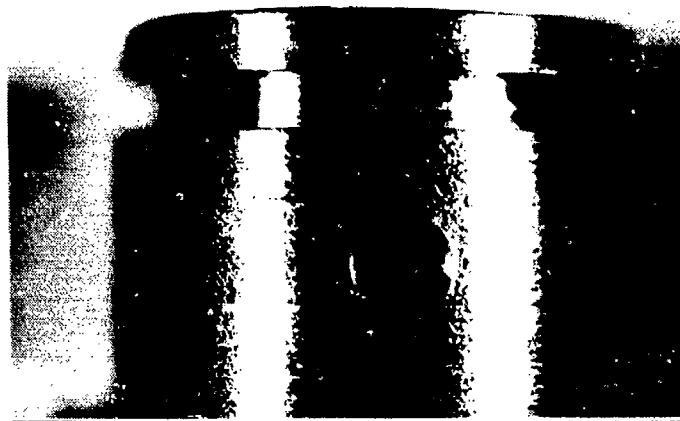
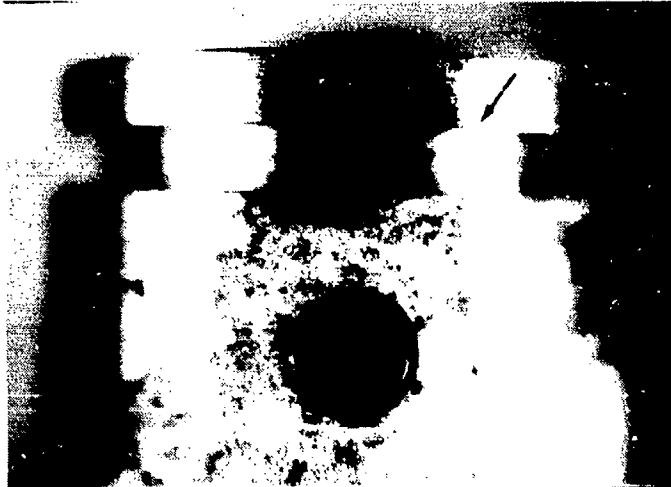


**FIGURE 18. 1018 STEEL/6061-T6 ALUMINUM VESSELS FABRICATED FOR CREVICE CORROSION TEST IN METHANOL**



(BEFORE)

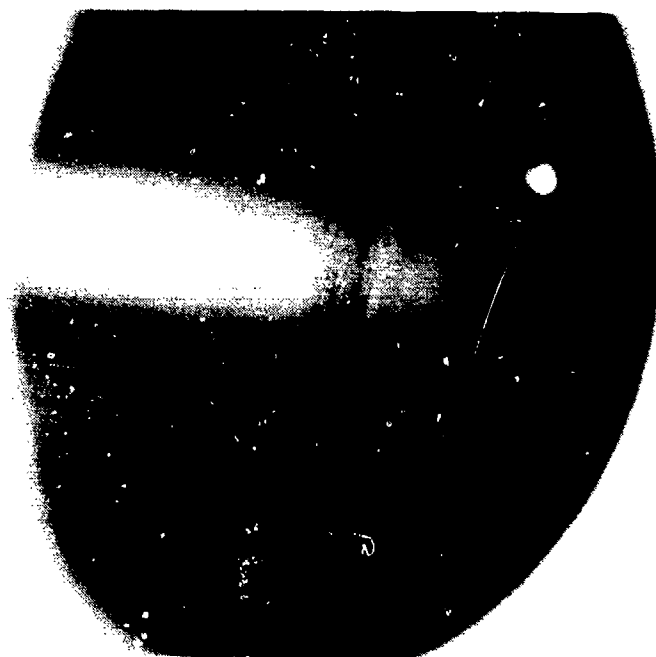


(AFTER ARGON FILL)



(AFTER AIR FILL)

FIGURE 19. ZINC-PLATED STEEL CAP, BEFORE AND AFTER CREVICE CORROSION TEST, ARGON FILL AND AIR FILL



(BEFORE)



(AFTER)

**FIGURE 20. O-RING CONTACT AREA OF UNANODIZED 6061-T6 ALUMINUM CONTAINER, BEFORE AND AFTER CREVICE CORROSION TEST**

## 2. Suitability of the ethylene-propylene O-rings:

- a. Compatibility of the O-ring material with the fuel
- b. Alternative O-ring materials
- c. Long term fuel leakage, internal and external
- d. Effect of storage temperature

The issues under 2. are marginally within the scope of such a test as noted above. However, these were of major concern to this project because of the requirement of lengthy device storage life and flammability danger on leakage. Therefore, they are addressed in so far as possible.

During the first phase of this study, short term compatibility of the fuel mixture with the ethylene-propylene O-ring was established by a short term elevated temperature (20 minute boiling) and extended (2.5 day ambient) immersion tests. Table 4 indicates the degree of compatibility of various elastomers with methanol. Ethylene-propylene is listed here under its trade name of NORDEL<sup>tm</sup>. Although methanol is listed as having little or no effect on this material at the test temperature, the caution expressed in the underlined paragraph at the top of this table may be especially pertinent to the present case.

There was legitimate question of the long term suitability of the ethylene-propylene material in the fluid. An alternative recommendation of neoprene was made. The data of Table 4 lists the latter also as having good chemical resistance to methanol. Material properties given in Table 5, however, do not necessarily support this recommendation. With the exception of the somewhat poorer performance of ethylene-propylene in solvents and petroleum based fluids than neoprene, the former appears to be superior in other important categories. This is true especially of the sustained service temperature parameter. This is listed as 95°C for neoprene and 145°C for ethylene-propylene. Hence, the necessity to make some judgement on the subject from the results of the present test.

The condition of the O-ring at termination of the sealed container test was a critical factor in this judgement. Qualitative evaluation based upon comparison of properties (e.g., swelling, stiffness, etc.) were made. The test period at elevated temperature is approximately equivalent to 5-6 years storage at ambient temperature.

TABLE 4. CHEMICAL RESISTANCE OF VARIOUS ELASTOMERS

# CHEMICAL RESISTANCE

of the Du Pont elastomers

Du Pont elastomers are used widely and successfully in contact with a broad variety of chemicals. To assist engineers in selecting the appropriate elastomer for the particular environment, the accompanying tabulation has been prepared. We emphasize that it should be used as a guide only. The tabulation is based in part on laboratory tests and records of actual service performance and in part on experienced judgment.

But an elastomer's degree of compatibility with a particular fluid also depends on such variables as temperature, aeration, velocity of flow, duration of exposure, stability of the fluid, degree of contact, etc. Therefore, it is always advisable to test the material under actual service conditions before specification. If this is not practical, tests should be designed that simulate service conditions as closely as possible.

Chemical	ANIPRENE*	HYTALON*	HYTREL*	Neoprene	NOREL*	VARAC*	VTOR*
Acetic acid	C	C		C	A	B	C
Acetic acid 10%	B	A	A	A	A	A	C
Acetic acid 30%	C	A	A	A	A	A	C
Acetic acid 50%	C	A	A	C	B	C	C
Acetic acid 60%							
Acetic acid 70%							
Acetic acid 80%							
Acetic acid 90%							
Acetic acid 100%							
Acetic acid 110%							
Acetic acid 120%							
Acetic acid 130%							
Acetic acid 140%							
Acetic acid 150%							
Acetic acid 160%							
Acetic acid 170%							
Acetic acid 180%							
Acetic acid 190%							
Acetic acid 200%							
Acetic acid 210%							
Acetic acid 220%							
Acetic acid 230%							
Acetic acid 240%							
Acetic acid 250%							
Acetic acid 260%							
Acetic acid 270%							
Acetic acid 280%							
Acetic acid 290%							
Acetic acid 300%							
Acetic acid 310%							
Acetic acid 320%							
Acetic acid 330%							
Acetic acid 340%							
Acetic acid 350%							
Acetic acid 360%							
Acetic acid 370%							
Acetic acid 380%							
Acetic acid 390%							
Acetic acid 400%							
Acetic acid 410%							
Acetic acid 420%							
Acetic acid 430%							
Acetic acid 440%							
Acetic acid 450%							
Acetic acid 460%							
Acetic acid 470%							
Acetic acid 480%							
Acetic acid 490%							
Acetic acid 500%							
Acetic acid 510%							
Acetic acid 520%							
Acetic acid 530%							
Acetic acid 540%							
Acetic acid 550%							
Acetic acid 560%							
Acetic acid 570%							
Acetic acid 580%							
Acetic acid 590%							
Acetic acid 600%							
Acetic acid 610%							
Acetic acid 620%							
Acetic acid 630%							
Acetic acid 640%							
Acetic acid 650%							
Acetic acid 660%							
Acetic acid 670%							
Acetic acid 680%							
Acetic acid 690%							
Acetic acid 700%							
Acetic acid 710%							
Acetic acid 720%							
Acetic acid 730%							
Acetic acid 740%							
Acetic acid 750%							
Acetic acid 760%							
Acetic acid 770%							
Acetic acid 780%							
Acetic acid 790%							
Acetic acid 800%							
Acetic acid 810%							
Acetic acid 820%							
Acetic acid 830%							
Acetic acid 840%							
Acetic acid 850%							
Acetic acid 860%							
Acetic acid 870%							
Acetic acid 880%							
Acetic acid 890%							
Acetic acid 900%							
Acetic acid 910%							
Acetic acid 920%							
Acetic acid 930%							
Acetic acid 940%							
Acetic acid 950%							
Acetic acid 960%							
Acetic acid 970%							
Acetic acid 980%							
Acetic acid 990%							
Acetic acid 1000%							

Chemical	ANIPRENE*	HYTALON*	HYTREL*	Neoprene	NOREL*	VARAC*	VTOR*
Acetic acid	C	C		C	A	B	C
Acetic acid 10%	B	A	A	A	A	A	C
Acetic acid 30%	C	A	A	A	A	A	C
Acetic acid 50%	C	A	A	C	B	C	C
Acetic acid 60%							
Acetic acid 70%							
Acetic acid 80%							
Acetic acid 90%							
Acetic acid 100%							
Acetic acid 110%							
Acetic acid 120%							
Acetic acid 130%							
Acetic acid 140%							
Acetic acid 150%							
Acetic acid 160%							
Acetic acid 170%							
Acetic acid 180%							
Acetic acid 190%							
Acetic acid 200%							
Acetic acid 210%							
Acetic acid 220%							
Acetic acid 230%							
Acetic acid 240%							
Acetic acid 250%							
Acetic acid 260%							
Acetic acid 270%							
Acetic acid 280%							
Acetic acid 290%							
Acetic acid 300%							
Acetic acid 310%							
Acetic acid 320%							
Acetic acid 330%							
Acetic acid 340%							
Acetic acid 350%							
Acetic acid 360%							
Acetic acid 370%							
Acetic acid 380%							
Acetic acid 390%							
Acetic acid 400%							
Acetic acid 410%							
Acetic acid 420%							
Acetic acid 430%							
Acetic acid 440%							
Acetic acid 450%							
Acetic acid 460%							
Acetic acid 470%							
Acetic acid 480%							
Acetic acid 490%							
Acetic acid 500%							
Acetic acid 510%							
Acetic acid 520%							
Acetic acid 530%							
Acetic acid 540%							
Acetic acid 550%							
Acetic acid 560%							
Acetic acid 570%							
Acetic acid 580%							
Acetic acid 590%							
Acetic acid 600%							
Acetic acid 610%							
Acetic acid 620%							
Acetic acid 630%							
Acetic acid 640%							
Acetic acid 650%							
Acetic acid 660%							
Acetic acid 670%							
Acetic acid 680%							
Acetic acid 690%							
Acetic acid 700%							
Acetic acid 710%							
Acetic acid 720%							
Acetic acid 730%							
Acetic acid 740%							
Acetic acid 750%							
Acetic acid 760%							
Acetic acid 770%							
Acetic acid 780%							
Acetic acid 790%							
Acetic acid 800%							
Acetic acid 810%							
Acetic acid 820%							
Acetic acid 830%							
Acetic acid 840%							
Acetic acid 850%							
Acetic acid 860%							
Acetic acid 870%							
Acetic acid 880%							
Acetic acid 890%							
Acetic acid 900%							
Acetic acid 910%							
Acetic acid 920%							
Acetic acid 930%							
Acetic acid 940%							
Acetic acid 950%							
Acetic acid 960%							
Acetic acid 970%							
Acetic acid 980%							
Acetic acid 990%							
Acetic acid 1000%							

Temperature Conversion  
°F. 100 104 112 120 122 130 150 158 176 200 212 220 225 230 250 270 280 288 300 350 382 400 428 450 550  
°C 38 40 45 49 50 54 58 70 80 83 100 104 107 110 121 132 138 141 148 177 200 204 220 232 288

Rating Key  
A—Fluid has little or no effect  
B—Fluid has minor to moderate effect  
C—Fluid has severe effect  
T—No data—likely to be compatible  
X—No data—not likely to be compatible  
Blanks indicate no evaluation has been attempted.

Unless otherwise noted, concentration of aqueous solutions are saturated.  
All ratings are at room temperature unless specified.

TABLE 5. COMPARATIVE PROPERTIES OF O-RING MATERIALS

## COMPARATIVE PROPERTIES

Property	Isopren Rubber	ADIPRENE <sup>®</sup> polyurethane	HYTALON <sup>®</sup> chloro- sulfonated poly- ethylene	HYTREL <sup>®</sup> polyester elastomer				Neopren chloroprene	MBREL <sup>®</sup> ethylene- propylene- diene polymer	BAMAC <sup>®</sup> ethylene / acrylic elastomer	WITON <sup>®</sup> co-polymer of vinylidene fluoride and hexafluoro- propylene
<b>HARDNESS RANGE (Shoremeter A&amp;D)</b>	30-90A	60-99+A (up to 80D)	40-95A	92A	55D	63D	72D	40-95A	40-90A	40-95A	55-95A
<b>TENSILE STRENGTH, MPa (psi)</b>	Over 20.7 (3,000)	Over 27.6 (4,000)	Over 17.2 (2,500)	25.5 (3,700)	44.1 (6,400)	40.0 (5,800)	40.0 (5,800)	Over 20.7 (3,000)	—	—	Over 12.4 (1,800)
<b>Block loaded clocks</b>	Over 20.7 (3,000)	—	Over 20.7 (3,000)	—	—	—	—	Over 20.7 (3,000)	Over 20.7 (3,000)	Over 17.2 (2,500)	Over 13.8 (2,000)
<b>SPECIFIC GRAVITY (from Material)</b>	0.93	1.06	1.12-1.28	1.17	1.20	1.22	1.25	1.23	0.86	1.08-1.12	1.85
<b>VULCANIZING PROPERTIES</b>	Excellent	Excellent	Excellent	Unnecessary to vulcanize				Excellent	Excellent	Good to Excellent	Good
<b>ADHESION TO METALS</b>	Excellent	Excellent	Excellent	Good	Good	Good	Good	Excellent	Good to Excel	V.G. to Excellent	Good
<b>ADHESION TO FABRICS</b>	Excellent	Excellent	Good	Good	Good	Good	Good	Excellent	Good	Good	Good to Excel
<b>TEAR RESISTANCE</b>	Good	Excellent	Fair	Excel.	Outstg.	Outstg.	Outstg.	Good	Good	Good	Fair
<b>ABRASION RESISTANCE</b>	Excellent	Outstanding	Excellent	Outstg.	Outstg.	Outstg.	Outstg.	Excellent	Excellent	Good	Good
<b>COMPRESSION SET</b>	Good	Fair	Fair	Fair	Fair	Fair	Fair	Fair to Good	Good	Good	Fair to Good
<b>DEFORMED</b>											
<b>Cold</b>	Excellent	Poor at V.L. temp.	Good	V. Good	Good	Fair	Fair	Very Good	Very Good	Poor	Good
<b>Hot</b>	Excellent	Good at R.T.	Good	Excel.	V. Good	Good	Good	Very Good	Very Good	Fair	Excellent
<b>DIELECTRIC STRENGTH</b>	Excellent	Excellent	Excellent	Fair to Good	Fair to Good	Fair to Good	Good	Good	Excellent	Good	Good
<b>ELECTRICAL INSULATION</b>	Good to Excellent	Fair to Good	Good	Fair to Good	Fair to Good	Fair to Good	Good	Fair to Good	Excellent	Fair to Good	Fair to Good
<b>PERMEABILITY TO GASES</b>	Fair	Fair	Low - V.L.	Good	Fair	Fair	Fair	Good	Low	Very Low	Very Low
<b>ACID RESISTANCE</b>											
<b>Solids</b>	Fair to Good	Fair	Excellent	Fair	Fair	Fair	Fair	Excellent	Excellent	Good	Excellent
<b>Concentrated</b>	Fair to Good	Poor	Very Good	Poor	Poor	Poor	Poor	Good	Excellent	Poor	Excellent
<b>SOLVENT RESISTANCE</b>											
<b>Aliphatic hydrocarbons</b>	Poor	Excellent	Good	Excel.	Excel.	Excel.	Excel.	Good	Poor	Good	Excellent
<b>Aromatic hydrocarbons</b>	Poor	Fair to Good	Fair	Good	Good	Good	Good	Fair	Poor	Fair	Excellent
<b>Oxygenated (ketones, etc.)</b>	Fair to Good	Poor	Poor	Fair	Good	Good	Good	Poor	Good	Poor	Poor
<b>Longer solvents</b>	Poor	Poor	Poor	Fair	Fair to Good	Good	Good	Poor	Poor	Poor	Poor
<b>RESISTANCE TO:</b>											
<b>Swelling in lubricating oil</b>	Poor	Excellent	Excel.	Good	Excel.	Excel.	Excel.	Good	Poor	Good	Excellent
<b>Oil and gasoline</b>	Poor	Excellent	Good	Very Good	Excel.	Excel.	Excel.	Good	Poor	Good	Excellent
<b>Animal and vegetable oils</b>	Poor to Good	Excellent	Good	Very Good	Excel.	Excel.	Excel.	Good	Good	Good	Excellent
<b>Water absorption</b>											
	Very Good	Good at R.T. Poor at 100°C (212°F)	Very Good	V. Good up to 100°C (212°F)	V. Good up to 100°C (212°F)	V. Good up to 100°C (212°F)	V. Good up to 100°C (212°F)	Good	Very Good	Very Good up to 100°C (212°F)	Very Good
<b>Oxidation</b>	Good	Excellent	Excellent	Excel.	Excel.	Excel.	Excel.	Excellent	Excellent	Outstanding	Outstanding
<b>Stress</b>	Fair	Excellent	Outstanding	Excel.	Excel.	Excel.	Excel.	Excellent	Outstanding	Outstanding	Outstanding
<b>Long-term aging</b>	Poor	Good	Outstanding	Good***	Good***	Good***	Good***	Very Good	Outstanding	Outstanding	Outstanding
<b>Heat aging (upper limit cool service)</b>	85°C (185°F)	85°C (185°F)	135°C (275°F)	100°C (212°F)	110°C (230°F)	110°C (230°F)	110°C (230°F)	95°C (203°F)	145°C (293°F)	165°C (323°F)	205°C (401°F)
<b>Flame**</b>	Poor	Fair (will melt)	Good	Good*** (will melt)				Very Good	Poor	Poor	Excellent
<b>Heat</b>	Good	Good	Excellent	V. Good	Excel.	Excel.	Excel.	Very Good	Excellent	Excellent	Outstanding
<b>Cold</b>	Excellent	Excellent	Good	Excel.	Excel.	Excel.	Excel.	Good	Excellent	Good	Good

(Data of Tables 4 and 5 obtained from bulletin entitled, "Engineering Guide to the duPont Elastomers," E. I. DuPont de Nemours & Co., Inc., Elastomers Division, Wilmington, DE 19898.)

## RESULTS

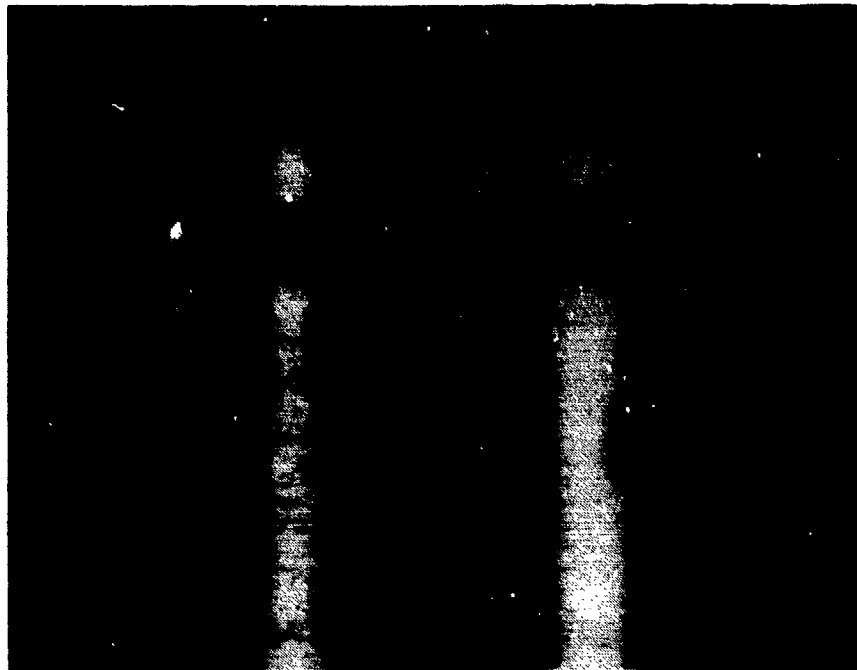
Figure 19(middle) pictures the O-ring groove area of the surface treated, inert atmosphere vessel at the test conclusion. Figure 19(bottom) shows the same portion of the container filled in air. Comparison of these photographs indicates no corrosion or removal of zinc plating from the fuel contacting upper edge (arrow) of the O-ring groove in either case. Apparently insufficient free oxygen is present, even with air filling, to produce any corrosion. Also apparently, no decomposition of the fuel has taken place as a source of additional free oxygen for corrosion propagation.

An initially unanticipated result of the test, however, is the corrosion observed on the lower portion (in Figure 19 photographs) of the caps. This is the atmosphere exposed side of the seal. This corrosion was caused by water seepage or condensation in the containing jar and subsequently into the crevice between cap and container bottom. The corrosion here has apparently oxidized the zinc plating. It has made its way to the very edge of the O-ring groove. The attack here appears to be confined at this point in time to the zinc coating because of its sacrificial nature.

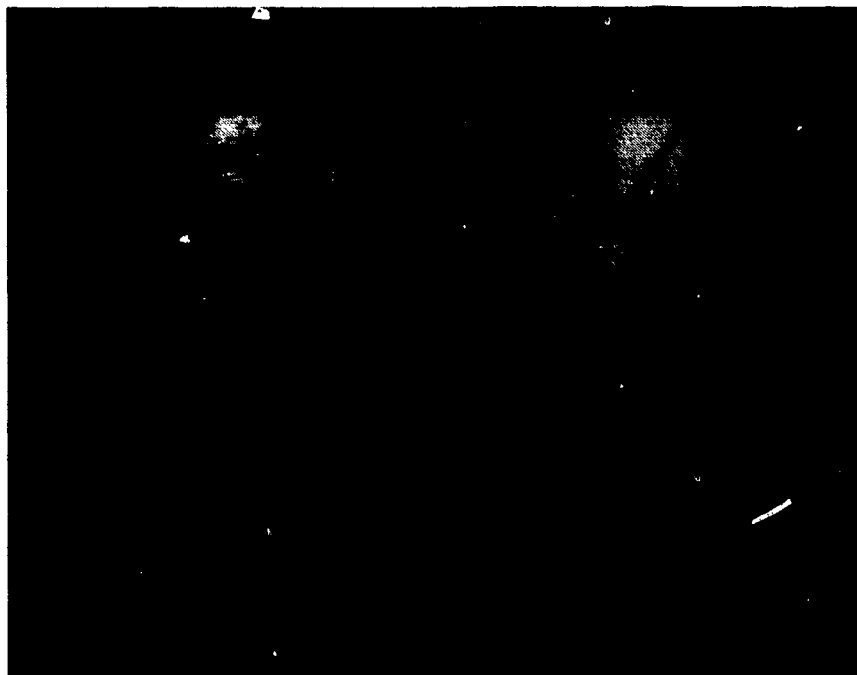
Figure 21 shows the situation with one of the untreated tops. Likewise, in this case, no corrosion has occurred on the fuel contacting portion of the O-ring groove (arrow at top of lower photo). On the other hand, extensive corrosion has taken place on the atmosphere side up to the edge of the groove. The corrosion is not yet so serious as to cause any leakage. It should be noted, however, that this degree of corrosion has been produced by limited contact with the tap water of the constant temperature bath. Extensive exposure to seawater could produce a much worse condition.

Returning to Figure 20, the lower photograph shows the aluminum container at the O-ring contact region after the test. No crevice corrosion or pitting is evident. The noteworthy detail is the black streak of O-ring material visible in the lower photograph. This indicates the degree of softening of the O-ring which has taken place. The subject of O-ring material choice has been discussed above and should be viewed in light of the results given below and anticipation of extended device storage.

Before opening at the test conclusion, each container was weighed to determine the extent of leakage of fuel during the test. Table 6 indicates the results of these measurements. The initial, final and empty container weights are indicated. The percent losses noted in the last column are quite low, given the severity of the test. A portion of these losses, in fact, can be attributed to fuel vapor absorption into the O-rings.



(BEFORE)



(AFTER)

FIGURE 21. UNPLATED 1081 STEEL CAP BEFORE AND AFTER CREVICE CORROSION TEST

TABLE 6. ELECTROLYTE LOSS DURING 70°C CREVICE CORROSION TEST

<u>VESSEL ID</u>	<u>INIT. WT.(g)</u>	<u>FIN. WT.(g)</u>	<u>MT WT.(g)</u>	<u>% FUEL LOSS</u>
Anod/Zn pl Ar fill	132.011	130.59	123.03	16
Anod/Zn pl Air fill	133.191	132.90	124.00	3.2
Untreated Ar fill	132.261	131.79	122.95	5.1
Untreated Air fill	131.321	130.78	121.70	5.6

The evidence of Figure 20 shows that the O-ring has undergone at least some softening in the course of this test. The post-test O-ring dimensions of about 0.65" ring X-section and 0.745" ring diameter were very close to those of an untested O-ring. Simple handling, however, showed the tested rings to be in a much less resilient and weakened state. A simple hanging weight test was used to document their loss in elasticity. A 670 gram weight was suspended from a ring stand by an untested (control) O-ring and then by each tested ring in turn. The length of stretch was measured in each case. The results are shown in Table 7.

TABLE 7. SOFTENING OF O-RING DURING 70°C CREVICE CORROSION TEST

<u>IDENTIFICATION</u>	<u>STRETCHED LNTH.</u>	<u>% INCREASE</u>
(Unstretched length in each case = 1 inch)		
Untested (control)	1.325"	32.5
Unplated, air fill	2.34"	234
Unplated, Ar fill	2.58"	258
Zn plated, air fill	2.38"	238
Zn plated, Ar fill	2.60"	260

One significant conclusion to be drawn from this check is that the vessels have sustained only slight leakage during the test period. Fluid losses ranged from 3-16% of the contents. While this finding does not assure that any internal leakage definitely will not occur at the small O-ring between fuel cavity and gas generator, the probability of serious leakage over a five year storage period is small with the current O-ring material. Marked softening and weakening of the ring, however, did occur during the test. This casts doubt on seal integrity over a more prolonged storage period. The situation may warrant the testing of other O-ring materials as had been recommended.

## CHAPTER 6

## SUMMARY

Potentiodynamic scanning of mounted test sample of 6061-T6 aluminum immersed only a few minutes in the methanolic fuel mixture containing  $\text{CCl}_4$  initiated very severe autocatalytic pitting. The pitting apparently initiates spontaneously at somewhat elevated temperatures after a certain induction period. This fuel was deemed incompatible with the device materials and further tests with it were suspended.

Pure methanol displayed a much more moderate behavior. There was no pitting or other serious corrosion of the anodized aluminum cavity surface subjected to a similar regime of pd scanning as above. A uniform corrosion rate of the order of 1-10 mils/year was measured. The limited data showed evidence of surface passivation. The plated steel surface showed some discoloration, probably due to dissolution of portions of the zinc coating. A non-anodized (polished) aluminum surface showed some pitting under similar conditions of exposure to the pure methanol. There was no indication, however, of very severe autocatalytic attack.

A galvanic couple corrosion test of anodized 6060-T6 aluminum and zinc plated 1018 steel made over a six week period in pure methanol showed a very low corrosion rate ( $<.001$  mil/year) and complete absence of pitting in either metal. The zinc plating on the steel component acted as sacrificial anode over the first 400 hours. Thereupon, the aluminum became the anodic (corroding) member. The corrosion current density gradually increased and finally became constant at about 1 nanoamp/cm<sup>2</sup>. This corresponds to the low rate noted above.

The sealed container crevice corrosion test revealed no evidence of corrosion in the O-ring groove area due to contact with methanol at 70°C over the three month test period. This remained true even for the unplated/unanodized vessels and for vessels filled in air. There was no evidence of fuel breakdown. The test did reveal the possibility of corrosion on the atmosphere exposed side of the O-ring groove. This was caused, in the test, by infiltration of condensation or thermal bath water into the crevice between container and cap. This corrosion could become severe in the case of repeated wetting with seawater.

The scale vessels showed only small leakage over the elevated temperature accelerated corrosion test period. This was equivalent to about 5 years service under ambient conditions. Of potential concern, however, was the marked softening and weakening of the O-ring during the test. This indicates that device performance could be jeopardized by a longer storage period with the current O-ring material.

REFERENCES

1. Roques, Y., Mankowski, G., et al., Corrosion-NACE, Vol. 40, No. 10, Oct 1984, p. 561ff.
2. Singh, D. D. N. and Banerjee, M. K., Corrosion-NACE, Vol. 42, No. 3, Mar 1987.
3. LaQue, F. L. and Copson, H. R., Editors, Corrosion Resistance of Metals and Alloys, Second Edition, Reinhold Publishing Corporation, NY, 1963, p. 217.
4. Uhlig, H. H., Corrosion and Corrosion Control: An Introduction to Corrosion Science and Engineering, Second Edition, John Wiley and Sons, Inc., NY, 1971, pp. 300-01.

## DISTRIBUTION

	<u>Copies</u>		<u>Copies</u>
Office of Naval Research		Department of the Army	
Attn: Code 1131 (S. Fishman)	2	Attn: DRXMR-MMC (A. Levitt)	1
800 North Quincy Street		Building 39	
Arlington, VA 22217		Watertown, MA 02712	
Office of the Deputy		Naval Research Laboratory	
Undersecretary of Defense		Attn: Code 6372 (R. Crowe)	1
Attn: J. Persh	1	E. McCafferty	1
Staff Specialist for Materials		P. Trzaskoma	1
Washington, DC 20301		P. Natishan	1
Defense Advanced Research		Washington, DC 20375	
Attn: P. Parrish	1	Chief of Naval Research	
1400 Wilson Blvd.		Office of Navy Technology	
Arlington, VA 22209		Attn: Code 0725 (J. J. Kelly)	1
Commander		Code 431 (A. J. Sedriks)	1
Naval Ocean Systems Center		Washington, DC 20360	
Attn: Code 903 (P. D. Burke)	1	Defense Technical Information	
Code 932 (J. Maltby)	1	Center	
San Diego, CA 92152		Cameron Station	
Commander		Alexandria, VA 22304-6145	12
Naval Sea Systems Command		Library of Congress	
Attn: SEA 05M1 (S. Rodgers)	1	Attn: Gift & Exchange Division	4
SEA 05M1 (H. Bliele)	1	Washington, DC 20540	
SEA 62D (A. Schweber)	1	Commander	
PMS 400C52 (V. Saige)	1	David Taylor Naval Ship Research	
Washington, DC 20362-5101		and Development Center	
Commander		Attn: Code 2813 (T. Morton)	1
Naval Air Development Center		Code 2813 (H. Hack)	1
Attn: Code 6062 (V. Agarwala)	1	Code 2813 (J. Scully)	1
Code 6062 (J. Thompson)	1	Annapolis, MD 21402	
Warminster, PA 18975000			

## DISTRIBUTION (Cont.)

	<u>Copies</u>		<u>Copies</u>
Commanding Officer		Internal Distribution:	
Naval Underwater Systems		E231	2
Center		E232	15
Attn: B. Sanoman	1	E342 (GIDEP)	1
Newport, RI 02840		G20	1
		G30	1
Commanding Officer		R32 (Ferrando)	10
Naval Ship Weapon Systems		R32 (Tydings)	5
Engineering Station		R32 (Hoover)	1
Attn: Code 4B06		R33 (Le)	1
(M. Scaturro)	1	R33 (McIntyre)	1
Port Hueneme, CA 93043		R33 (Dacres)	1
		R33 (Vasanth)	1
Commanding Officer		R33 (Sutula)	1
Naval Ship Systems		R35 (Musselman)	1
Engineering Station			
Attn: Code 053B			
(N. Clayton)	1		
Philadelphia Naval Base			
Philadelphia, PA 19112			
Novamet			
Attn: B. Schelling	2		
681 Laulins Road			
Wycoff, NJ 07481			